nature immunology

ARTICLES

https://doi.org/10.1038/s41590-018-0068-4

Recognition of microbial viability via TLR8 drives T_{FH} cell differentiation and vaccine responses

Matteo Ugolini[1,16], Jenny Gerhard[1,16], Sanne Burkert[2,16], Kristoffer Jarlov Jensen[3,4], Philipp Georg[1], Friederike Ebner[5], Sarah M. Volkers[1], Shruthi Thada[2,6], Kristina Dietert[7], Laura Bauer[8], Alexander Schäfer[9], Elisa T. Helbig[1], Bastian Opitz[1,10], Florian Kurth[1], Saubashya Sur[2], Nickel Dittrich[2], Sumanlatha Gaddam[6,11], Melanie L. Conrad[12], Christine S. Benn[3,13], Ulrike Blohm[9], Achim D. Gruber[7], Andreas Hutloff[8], Susanne Hartmann[5], Mark V. Boekschoten[14], Michael Müller[14,15], Gregers Jungersen[4], Ralf R. Schumann[2], Norbert Suttorp[1,10] and Leif E. Sander[1,10]*

Live attenuated vaccines are generally highly efficacious and often superior to inactivated vaccines, yet the underlying mechanisms of this remain largely unclear. Here we identify recognition of microbial viability as a potent stimulus for follicular helper T cell (T_{FH} cell) differentiation and vaccine responses. Antigen-presenting cells (APCs) distinguished viable bacteria from dead bacteria through Toll-like receptor 8 (TLR8)-dependent detection of bacterial RNA. In contrast to dead bacteria and other TLR ligands, live bacteria, bacterial RNA and synthetic TLR8 agonists induced a specific cytokine profile in human and porcine APCs, thereby promoting T_{FH} cell differentiation. In domestic pigs, immunization with a live bacterial vaccine induced robust T_{FH} cell and antibody responses, but immunization with its heat-killed counterpart did not. Finally, a hypermorphic *TLR8* polymorphism was associated with protective immunity elicited by vaccination with bacillus Calmette-Guérin (BCG) in a human cohort. We have thus identified TLR8 as an important driver of T_{FH} cell differentiation and a promising target for T_{FH} cell–skewing vaccine adjuvants.

Live attenuated microbes represent the first generation of vaccines and have contributed to the extinction of, or a substantial reduction in, deadly diseases such as smallpox or rabies[1–3]. The unparalleled success of live vaccines is based on empiricism[4], yet their exact mechanisms of action, their frequently observed superiority over inactivated vaccine preparations[5] and their exceptional ability to induce protective, often lifelong, immunity still remain largely unexplained. The innate immune system detects microbial invaders and carefully determines the level of infectious threat in order to elicit appropriate, well-measured immune responses[6]. Mouse innate immune cells possess an inherent ability to discriminate live microorganisms from dead microorganisms[7]. Viable and thus potentially harmful microorganisms contain pathogen-associated molecular patterns (PAMPs) specific for live microbes. Bacterial mRNA has been identified as such a viability-associated PAMP ('vita-PAMP'), the detection of which elicits distinct inflammatory immune responses and promotes humoral immunity in mice[7]. However, the role of vita-PAMPs and their receptors in regulating human immune responses remains unknown.

Given the importance of innate immune signals in shaping adaptive immune responses[8], we sought to determine whether recognition of bacterial viability by the innate immune system affects the ensuing helper T cell responses and, in particular, the differentiation of T_{FH} cells. T_{FH} cells are pivotal regulators of the germinal-center response and humoral immunity[9,10], and intense research has unraveled the complexity of the development of T_{FH} cells and their interactions with B cells[10–14]. However, the early stages of T_{FH} cell differentiation and the role of APC-derived innate immune signals in controlling this process, especially in humans, have remained unclear. Targeted mobilization of T_{FH} cell responses poses a major hurdle for vaccine development. Therefore, the identification of particular innate immune pathways with T_{FH} cell–skewing ability in humans would be highly desirable for the rational design of T_{FH} cell–targeted vaccine adjuvants.

[1]Department of Infectious Diseases and Pulmonary Medicine, Charité–Universitätsmedizin Berlin, corporate member of Freie Universität Berlin, Humboldt-Universität zu Berlin, and Berlin Institute of Health, Berlin, Germany. [2]Institute of Microbiology and Hygiene, Charité–Universitätsmedizin Berlin, corporate member of Freie Universität Berlin, Humboldt-Universität zu Berlin, and Berlin Institute of Health, Berlin, Germany. [3]Research Center for Vitamins and Vaccines, Bandim Health Project, Statens Serum Institut, Copenhagen, Denmark. [4]Department of Biotechnology and Biomedicine, Technical University of Denmark, Kgs Lyngby, Denmark. [5]Department of Veterinary Medicine, Institute of Immunology, Freie Universität Berlin, Berlin, Germany. [6]Bhagwan Mahavir Medical Research Centre, Hyderabad, India. [7]Department of Veterinary Medicine, Institute of Veterinary Pathology, Freie Universität Berlin, Berlin, Germany. [8]Chronic Immune Reactions, German Rheumatism Research Centre, a Leibniz Institute, Berlin, Germany. [9]Institute of Immunology, Friedrich-Loeffler-Institut, Federal Research Institute for Animal Health, Greifswald—Island of Riems, Germany. [10]German Center for Lung Research (DZL), Berlin, Germany. [11]Department of Genetics, Osmania University, Hyderabad, India. [12]Department of Internal Medicine and Dermatology, Division of Psychosomatic Medicine, Charité–Universitätsmedizin Berlin, corporate member of Freie Universität Berlin, Humboldt-Universität zu Berlin, and Berlin Institute of Health, Berlin, Germany. [13]Odense Patient Data Explorative Network (OPEN), Odense University Hospital/Department of Clinical Research, University of Southern Denmark, Odense, Denmark. [14]Nutrition, Metabolism and Genomics Group, Division of Human Nutrition, Wageningen University, Wageningen, The Netherlands. [15]Norwich Medical School, University of East Anglia, Norwich, UK. [16]These authors contributed equally: Matteo Ugolini, Jenny Gerhard and Sanne Burkert. *e-mail: leif-erik.sander@charite.de

In this study, we found that human APCs distinguished viable bacteria from dead bacteria independently of virulence, by virtue of TLR8-dependent detection of bacterial RNA. The recognition of bacterial viability by the innate immune system led to transcriptional remodeling in human APCs and induced T_{FH} cell–promoting signals, most importantly interleukin 12 (IL-12). Activation of TLR8 by live bacteria, bacterial RNA or synthetic agonists promoted the differentiation of fully functional T_{FH} cells, whereas killed bacteria or other TLR agonists and adjuvants failed to do so. In domestic pigs, we observed robust T_{FH} cell and antibody responses following immunization with a commonly used vaccine containing live attenuated *Salmonella* but not following immunization with the same vaccine containing a heat-killed version of the *Salmonella*. Moreover, a case-control study revealed a strong association of a hypermorphic *TLR8* polymorphism with BCG-induced protection from infection with *Mycobacterium tuberculosis*, which linked function to protective immunity in response to a live attenuated vaccine in humans. In summary, we identified recognition of bacterial viability as a conserved innate immune checkpoint that preferentially promoted T_{FH} cell differentiation and humoral immunity.

Results

Detection of live bacteria promotes T_{FH} cell differentiation. In order to assess the contribution of innate immune signals to the differentiation of human T_{FH} cells, we co-cultured human $CD14^+CD16^-$ monocytes (as APCs) with autologous naive $CD4^+$ T cells isolated by negative selection of $CD45RO^+CD4^+$ T cells. APCs were stimulated with either live avirulent thymidine-auxotrophic (*thyA*$^-$; replication-defective) *Escherichia coli* (called 'EC' here)[7] or a heat-killed version of the same *E. coli* (HKEC). We chose avirulent auxotrophic bacteria to selectively analyze the effect of bacterial viability without the confounding effects of virulence factors and bacterial replication[7]. Following 90 min of stimulation of human $CD14^+CD16^-$ monocytes with EC or HKEC, naive $CD4^+$ T cells were added, together with antibiotics, and helper T cell differentiation was assessed 5 d later. Notably, EC-stimulated APCs induced naive $CD4^+$ T cells to produce large amounts of IL-21 and interferon-γ (IFN-γ), which are characteristic cytokines of T_{FH} cells and the T_H1 subset of helper T cells, respectively (Fig. 1a,b). This response was almost completely absent in cultures with APCs stimulated with HKEC or medium alone (Fig. 1a,b). T cell proliferation rates were similar in all conditions, and IL-17 was produced in moderate amounts regardless of bacterial viability (Fig. 1a,b). In line with the increased IL-21 production, stimulation with EC promoted the expression of the T_{FH} cell markers CXCR5, ICOS and PD-1, but stimulation with HKEC did not[15–17] (Fig. 1c,d and Supplementary Fig. 1a).

The transcription factor BCL-6 is required for successful development of T_{FH} cells[11,12]. APCs stimulated with EC induced co-expression of BCL-6 and IL-21 in $CD4^+$ T cells, as assessed by flow cytometry, whereas APCs stimulated with killed bacteria failed to do so (Fig. 1e,f). The expression of mRNA encoding the transcription factors T-bet and GATA-3 was downregulated in T cells incubated with APCs stimulated with EC or HKEC, relative to such expression in T cells activated with unstimulated APCs, whereas expression of mRNA encoding the transcription factors RORγt and Maf was slightly increased by the incubation of T cells with APCs stimulated with either EC or HKEC, as measured by hybridization-based multiplexed gene-expression quantitation (Fig. 1g and Supplementary Fig. 1b). The specific induction of T_{FH} cells upon sensing of live EC by the innate immune system was not specific to $CD14^+CD16^-$ monocytes, as similar results were obtained with primary human $CD1c^+$ myeloid dendritic cells (DCs) as APCs (Fig. 1h,i).

In order to assess the functionality of newly generated T_{FH} cells as true helpers of B cells, we sorted $CD4^+CD45RA^-CXCR5^+$ T_{FH} cells from the APC–T cell co-culture system at day 5 and compared them with naive $CD4^+CD45RA^+CXCR5^-$ T cells sorted from the blood of the same donor, assessing their ability to promote plasma-cell differentiation when co-cultured with heterologous tonsillar memory B cells. $CXCR5^+$ T_{FH} cells induced by EC-stimulated APCs promoted robust differentiation of $CD27^{hi}CD38^+$ plasma cells, while naive $CXCR5^-$ T cells from the same donor failed to do so (Fig. 1j,k). In addition, $CXCR5^+$ T_{FH} cells stimulated robust production of immunoglobulin G (IgG), which was not observed with naive T cells or in B cell–only cultures (Fig. 1l). $CXCR5^-$ T cells sorted from the co-cultures at day 5 provided weaker help than did $CXCR5^+$ T cells (Supplementary Fig. 1c–f). Collectively, these results indicated that the recognition of bacterial viability by human APCs of the innate immune system elicited potent differentiation signals for the generation of fully functional T_{FH} cells.

Recognition of bacterial viability modulates the cytokine profile of human APCs. In order to characterize the innate immune signals that control T_{FH} cell programming after the recognition of bacterial viability, we compared the transcriptome of $CD14^+CD16^-$ monocytes in response to live bacteria with that in response to dead bacteria. Detection of either EC or HKEC led to similar regulation of 1,051 transcripts in human monocytes (Fig. 2a), which indicated substantial similarity between the two stimuli, both of which contain an abundance of PAMPs and thereby engage a multitude of pattern-recognition receptors[7]. We detected a set of 193 genes that were regulated differentially in $CD14^+CD16^-$ monocytes in response to EC relative to their regulation in response to HKEC, including genes encoding the inflammatory cytokines TNF (*TNF*) and IL-12p40 (*IL12B*) (Fig. 2a,b and Supplementary Table 1). Accordingly, we detected release of IL-12 and TNF (assessed by ELISA) nearly exclusively in response to EC, not in response to HKEC, whereas the cytokines IL-6, IL-10, IL-23 and GM-CSF were produced regardless of bacterial viability (Fig. 2c).

Our finding of differential expression of IL-12 and TNF was in contrast to published observations of mouse macrophages and DCs, which produce large amounts of TNF and IL-12 in response to either live bacteria or killed bacteria or purified bacterial cell-wall components[7]. Similar to results obtained for mouse macrophages and DCs[7], release of IL-1β was induced by EC, but not by HKEC, in human monocytes (Fig. 2c), indicative of inflammasome activation. Production of TNF and IL-12 could not be restored by higher doses of HKEC (Fig. 2d). Other bacterial species, including avirulent Gram-positive *Bacillus subtilis*, as well as BCG (an attenuated strain of *Mycobacterium bovis* and widely used live vaccine against tuberculosis (TB)), elicited comparable cytokine patterns (Fig. 2e), which indicated that the response to bacterial viability was conserved and was largely independent of features specific to the bacterial species. Both EC and HKEC induced similar upregulation of the expression of maturation markers such as CD40 (Fig. 2f), which indicated intact innate recognition of both stimuli. Thus, human $CD14^+CD16^-$ monocytes discriminated precisely between live bacteria and dead bacteria independently of virulence or bacterial species, and they responded to bacterial viability with a distinct transcriptional program and cytokine profile.

'Viability-induced' T_{FH} cell responses are mediated by APC-derived IL-12. Next, we investigated whether APC-derived cytokines induced by the detection of live bacteria were driving the T_{FH} cell differentiation. $CD4^+$ T cells (isolated by negative selection from peripheral blood) showed high expression of IL-21 and BCL-6 and of CXCR5, ICOS and PD-1 when activated via CD3 and CD28 in the presence of supernatants of EC-stimulated $CD14^+CD16^-$ monocytes (Fig. 3a,b). Supernatants of HKEC-stimulated APCs did not induce a T_{FH} cell phenotype in $CD4^+$ T cells (Fig. 3a,b), while proliferation rates and IL-17 production were induced similarly by supernatants of EC-conditioned APCs and supernatants of HKEC-conditioned APCs (Supplementary Fig. 2a–c). These results

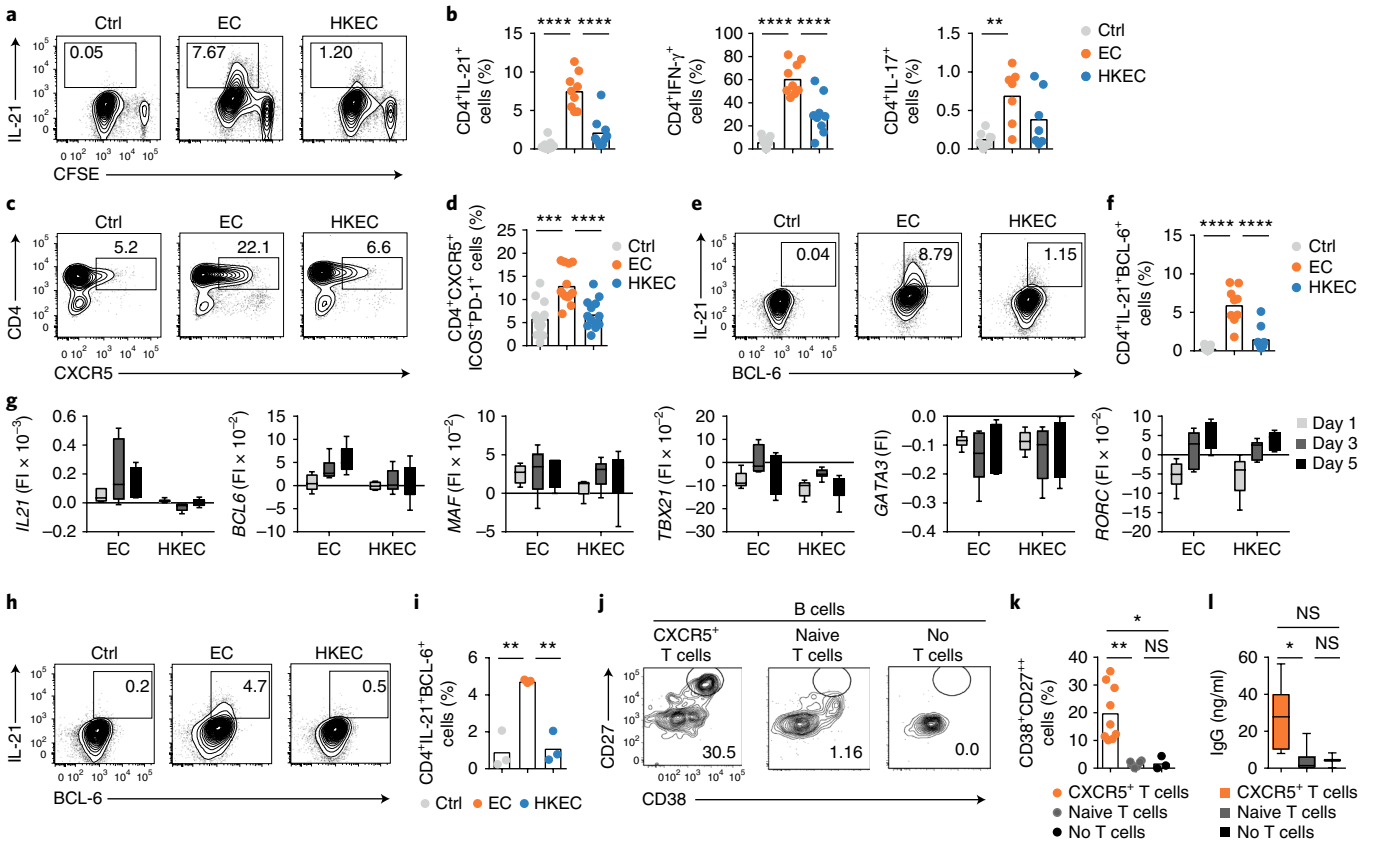

Fig. 1 | The recognition of live bacteria by the innate immune system promotes T_{FH} cell differentiation. a, Flow-cytometry analysis of the IL-21 expression and proliferation of autologous naive CD4+ T cells cultured for 5 d, in the presence of staphylococcal enterotoxin B (T cell antigen receptor stimulus in all T cell conditions), with human monocytes (as APCs) previously stimulated with medium (Ctrl), live EC or HKEC (above plots); proliferation was assessed as dilution of the division-tracking dye CFSE. **b**, Frequency of cytokine-positive CD4+ T cells in co-cultures as in **a** (key). **c**,**d**, Flow-cytometry analysis of the expression of CXCR5 (**c**), ICOS and PD-1 (Supplementary Fig. 1a) by T cells cultured as in **a** (above plots), and frequency of T cells positive for all three in such cultures (key) (**d**). **e**,**f**, Flow-cytometry analysis of the expression of IL-21 and BCL-6 by cells cultured as in a (above plots) (**e**), and frequency of IL-21+BCL-6+ cells in such cultures (key) (**f**). **g**, Fluorescent hybridization-based multiplex assay measuring the expression of genes encoding IL-21 (*IL21*) and the transcription factors BCL-6 (*BCL6*), Maf (*MAF*), T-bet (*TBX21*), GATA-3 (*GATA3*) and RORγt (*RORC*) in CD4+ T cells on day 1, 3 or 5 (key) of culture as in **a** (horizontal axis) ($n = 6$ donors), presented as corrected fluorescence intensity (FI), calculated by subtraction of the fluorescence intensity of the control sample at the same time point. **h**,**i**, Flow-cytometry analysis of the expression of IL-21 and BCL-6 by cells cultured as in **a** (above plots) but with CD1c+ myeloid DCs as APCs (**h**), and frequency of IL-21+BCL-6+ cells in such cultures (key) (**i**). **j**–**l**, Flow-cytometry analysis of the expression of CD27 and CD38 by tonsillar memory B cells cultured for 7 d alone (left) or with $CD4^+CD45RA^-CXCR5^+$ T_{FH} cells from day 5 of culture with EC-stimulated APCs as in **a** (left) or autologous naive $CD4^+CD45RA^+$ T cells from same donor (middle) (**j**), frequency of $CD38^+CD27^{hi}$ plasma cells in cultures as in **j** (key) (**k**) and ELISA of IgG in supernatants of cultures as in **j** (key) (**l**). Numbers adjacent to or in outlined areas (**a**,**c**,**e**,**h**,**j**) indicate percent cells in each throughout. Each symbol (**b**,**d**,**f**,**i**,**k**,**l**) represents an individual donor ($n = 9$ (IL-21), 9 (IFN-γ) or 7 (IL-17) (**b**); $n = 13$ (**d**); $n = 9$ (**f**); $n = 3$ (**i**); or $n = 9$ (CXCR5+ T cells), 9 (Naive T cells) or 3 (No T cells) (**k**,**l**)); error bars indicate maximum and minimum (**g**,**l**). NS, not significant ($P > 0.05$); $^*P < 0.05$, $^{**}P < 0.01$, $^{***}P < 0.001$ and $^{****}P < 0.0001$ (one-way analysis of variance (ANOVA) with post-hoc correction for multiple comparisons). Data are representative of one experiment per donor.

indicated a dominant role for APC-derived soluble factors in the initial stages of T_{FH} cell differentiation in response to live EC.

Various cytokines and cytokine combinations, including IL-21, IL-6, IL-27 and type I interferons, have been reported to promote T_{FH} cell differentiation in mice[9,18,19], whereas the differentiation of human T_{FH} cells is mediated mainly by the cytokines IL-12, IL-23 and TGF-β[10,20]. The cytokine requirements for vita-PAMP–induced human T_{FH} cell differentiation remain unclear. We found a strong correlation between the amount of IL-12 and TNF in supernatants of EC-stimulated APCs and the production of IL-21 by the activated T cells, whereas the amount of IL-6 in supernatants of APCs did not correlate with the production of IL-21 by T cells (Fig. 3c). The addition of a neutralizing antibody against IL-12 to the supernatants of EC-induced APCs almost completely abolished T_{FH} cell differentiation without affecting T cell proliferation rates (Fig. 3d–f and Supplementary Fig. 2a,d–f). Neutralization of IL-6 or IL-27 had no significant effect, whereas blockade of TNF partially inhibited T_{FH} cell differentiation, relative to such differentiation after the addition of isotype-matched control antibodies (Fig. 3d–f). Conversely, supplementing supernatants of unstimulated (control) APCs with recombinant IL-12 restored T_{FH} cell differentiation (Fig. 3d,e,g). Supplementation with recombinant TNF alone did not promote T_{FH} cell differentiation (Fig. 3g), which indicated that TNF might have a minor role or act in concert with IL-12 or other APC-derived factors. Neutralization of IL-1β in the supernatants of EC-induced APCs partially diminished T_{FH} cell differentiation, while supplementation of supernatants of unstimulated (control) APCs with recombinant IL-1β alone was insufficient to support T_{FH} cell differentiation (Supplementary Fig. 2d–f); this indicated that IL-1β might have additive effects in humans, consistent with published observations[20].

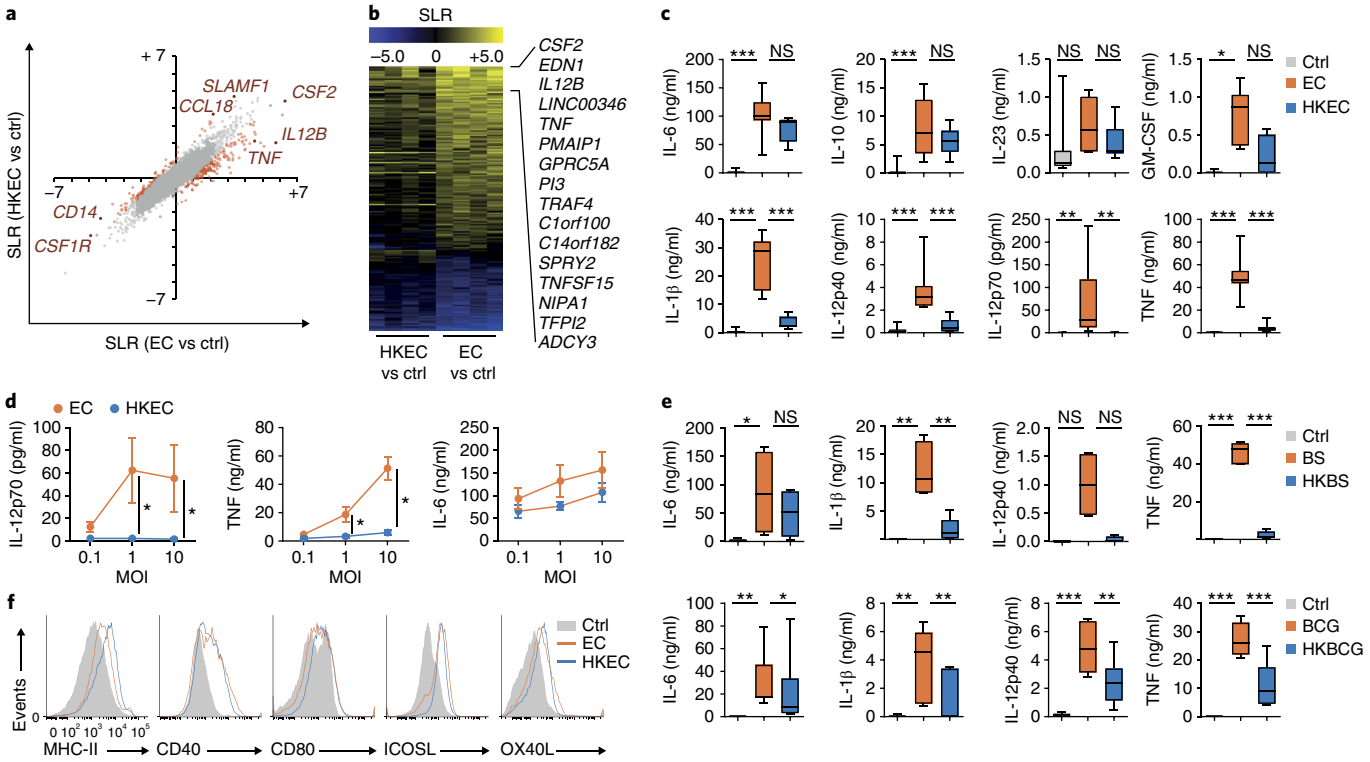

Fig. 2 | Detection of viable bacteria skews the cytokine profile of human monocytes. a, Genome-wide transcriptional analysis of human CD14$^+$CD16$^-$ monocytes ($n=4$ donors) stimulated for 6 h with medium (control (Ctrl)), EC or HKEC, presented as the mean signal log ratio (SLR) of each gene in EC-treated cells relative to that in control cells (EC vs Ctrl) plotted against that of HKEC-treated cells relative to that of control cells (HKEC vs Ctrl); red symbols indicate genes with a difference in SLR of >2 in EC-treated cells relative to that in HKEC-treated cells. **b**, Heat map of 193 genes with a change in SLR of >2 or ≤2 (key) in EC–versus–Ctrl compared with HKEC–versus–Ctrl as in **a** (below plot). **c**, Concentration of cytokines secreted by APCs ($n=3$–6 donors) left untreated (Ctrl) or stimulated for 18 h with EC or HKEC (key). **d**, Concentration of cytokines secreted by APCs ($n=4$ donors) stimulated with EC or HKEC (key) at an increasing multiplicity of infection (MOI) (horizontal axis). **e**, Concentration of cytokines secreted by APCs ($n=2$–5 donors (top row) or $n=4$ donors (bottom row)) that were left untreated (Ctrl) or stimulated with live *B. subtilis* (BS) or heat-killed *B. subtilis* (HKBS) (key) (top row) or with live *M. bovis* strain BCG (BCG) or heat-killed *M. bovis* strain BCG (HKBCG) (key) (bottom row). **f**, Flow-cytometry analysis of the surface expression of various markers on APCs ($n=5$ donors) at 18 h after treatment as in **c** (key). $^*P<0.05$, $^{**}P<0.01$ and $^{***}P<0.001$ (one-way ANOVA (**c**,**e**) or multiple *t*-tests with post-hoc correction for multiple comparisons (**d**)). Data are representative of four independent experiments (one per donor; **a**,**b**), three to six experiments (one per donor: $n=6$ (IL-1β and IL-12p70), $n=5$ (IL-6, IL-10, IL-12p40 and TNF), $n=4$ (IL-23) or $n=3$ (GM-CSF); (**c**), eight experiments (**d**; error bars, mean ± s.e.m.) or five experiments (top row) or four experiments (bottom row) (**e**) (error bars (**c**,**e**), maximum and minimum).

Blocking IFN-β or supplementation with recombinant IFN-β did not alter the differentiation of human T_{FH} cells (Supplementary Fig. 2d–f). Although membrane-bound mediators such as ICOSL[14] and OX40L[21] contribute to different stages of T_{FH} cell differentiation in vivo, we found no major difference in their surface expression on APCs stimulated with EC relative to that on APCs stimulated with HKEC (Fig. 2f), an observation that does not exclude the possibility of a role at later stages of differentiation. Thus, IL-12 was the critical innate immune signal produced in response to live bacteria to instruct early priming of T_{FH} cells in humans.

TLR8 is a vita-PAMP receptor that mediates IL-12 production and T_{FH} cell differentiation. In order to identify potential targets for T_{FH} cell–skewing adjuvants, we next investigated the nature of the innate immune receptor(s) and the ligands that elicited 'viability-induced' T_{FH} cell differentiation signals. We supplemented HKEC with various PAMPs and compared subsequent cytokine responses in CD14$^+$CD16$^-$ monocytes. Of the five different PAMPs tested here, only ligands of the endosomal single-stranded-RNA receptors TLR7 and TLR8 restored the production of IL-12 and TNF to levels comparable to those induced by EC (Fig. 4a). Inhibition of actin polymerization and phagocytosis via cytochalasin D, as well as blockade of endolysosomal acidification with bafilomycin A, abolished the EC-induced production of IL-12, but not that of IL-6 (Supplementary Fig. 3a), indicative of a role for endosomal receptors in the sensing of viable bacteria.

Since human monocytes expressed TLR8 but had only low expression of TLR7 (Supplementary Fig. 3b), and TLR8 recognizes bacterial RNA[22,23], we investigated whether TLR8 was the primary human vita-PAMP receptor for live bacteria. Endosomal delivery of bacterial RNA fully restored the production of TNF and IL-12 to levels comparable to those induced by EC and synthetic agonists of TLR7 and TLR8 (Fig. 4b) and induced upregulation of the expression of CD40, CD80 and other maturation markers (Supplementary Fig. 3c). Conversely, silencing the expression of the gene encoding TLR8 or the gene encoding its signaling adaptor MyD88 by RNA-mediated interference (with small interfering RNA (siRNA)) in CD14$^+$CD16$^-$ monocytes abolished the release of IL-12p70 and TNF in response to EC (Fig. 4c,d). The production of IL-6 was not affected by the silencing of either of those genes (Fig. 4c,d). In line with the proposed critical role for TLR8 as a vita-PAMP receptor, we found that ligation of TLR8 in APCs by the synthetic agonists CL075 or R848 potently promoted the differentiation of IL-21$^+$BCL-6$^+$ T_{FH} cells (Fig. 5a–c). In contrast, all other TLR ligands tested, including the licensed vaccine adjuvants MPLA (monophosphoryl lipid A; a TLR4 agonist) and CpG DNA (a TLR9 agonist), did not promote

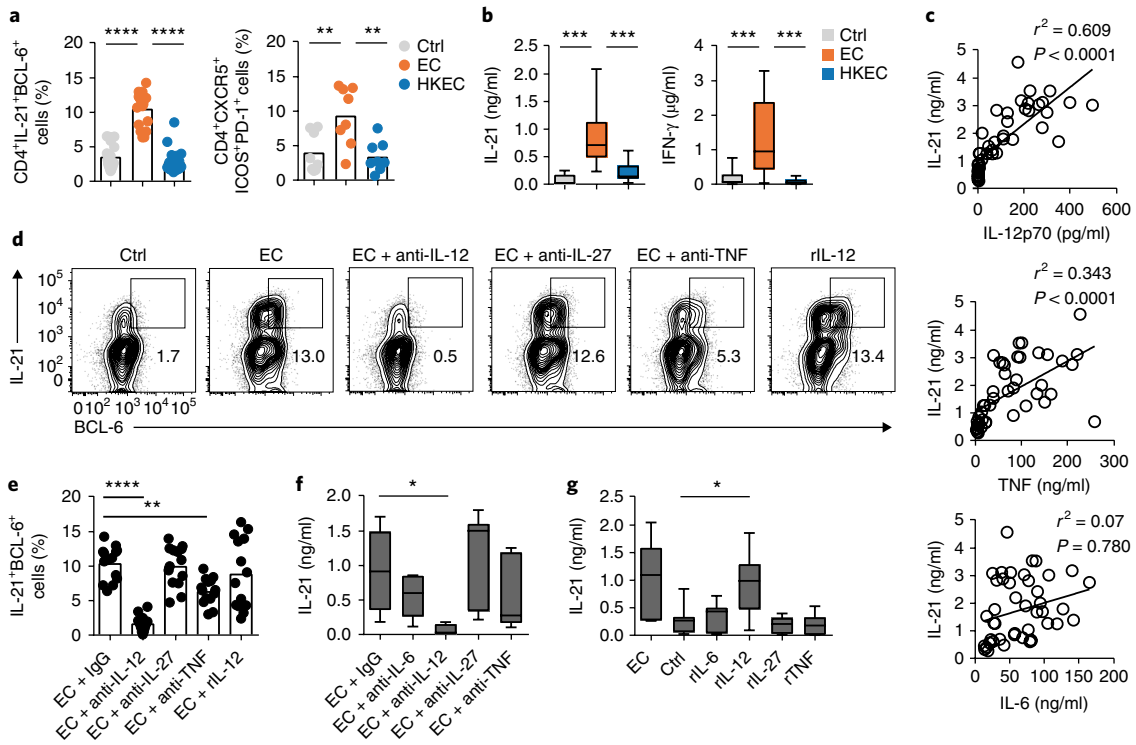

Fig. 3 | IL-12 is a critical signal for 'viability-induced' T_{FH} cell differentiation. a,**b**, Frequency of IL-21$^+$BCL-6$^+$ cells (left) or CXCR5$^+$ICOS$^+$PD-1$^+$ cells (right), assessed by flow cytometry (**a**), and ELISA of IL-21 (left) and IFN-γ (right) in supernatants (**b**) of CD4$^+$ T cells polyclonally activated by plate-bound antibody to CD3 and soluble antibody to CD28 in the presence of supernatants collected from APCs left unstimulated (Ctrl) or stimulated for 18 h with EC or HKEC (key) ($n = 19$ donors (IL-21$^+$BCL-6$^+$) or 8 donors (CXCR5$^+$ICOS$^+$PD-1$^+$) (**a**); or $n = 11$ donors (**b**)). **c**, Linear-regression analysis of the concentration of IL-21 produced by CD4$^+$ T cells versus that of IL-12p70 (top), TNF (middle) or IL-6 (bottom) in supernatants of APCs (samples from nine donors in five independent experiments; $n = 45$ (IL-12p70), 21(TNF) or 21 (IL-6)) in cultures as in **a**. **d**–**g**, Flow-cytometry analysis of the expression of IL-21 and BCL-6 (**d**), frequency of IL-21$^+$BCL-6$^+$ cells, assessed as in **d** (**e**) ($n = 14$), and ELISA of IL-21 in supernatants (**f**,**g**) ($n = 7$) of T cells cultured as in **a**,**b** with supernatants of EC-stimulated APCs in the presence or absence of the irrelevant control antibody IgG or neutralizing antibodies (anti-) or supernatants of control APCs supplemented with recombinant (r) cytokines (above plots (**d**) or horizontal axis (**e**–**g**)). Each symbol (**a**,**e**) represents an individual donor. $^*P < 0.05$, $^{**}P < 0.01$ and $^{***}P < 0.001$ (one-way ANOVA with post-hoc correction for multiple comparisons). Data are representative of 19 experiments (**a**,**b**), 45 experiments (**c**), 14 experiments (**d**,**e**) or 7 experiments (**f**,**g**) (error bars (**b**,**f**,**g**), maximum and minimum).

T_{FH} cell responses, even at high concentrations (Fig. 5a–c). Similar to its activation by live bacteria, the activation of TLR8 by purified bacterial RNA resulted in the robust differentiation of T_{FH} cells and their production of IL-21 (Fig. 5d,e), which demonstrated that the recognition of bacterial RNA by the innate immune system was a potent stimulator of T_{FH} cell–differentiation signals. Silencing *TLR8* expression in CD14$^+$CD16$^-$ monocytes diminished their ability to promote T_{FH} cell differentiation in response to EC, relative to the corresponding ability of EC-stimulated monocytes treated with control siRNA with a scrambled sequence (Fig. 5f,g). Collectively, these results identified TLR8 as the key sensor for bacterial viability in human APCs and a critical driver of IL-12 production and subsequent T_{FH} cell responses.

Recognition of bacterial viability is conserved in porcine APCs. Domestic pigs (*Sus scrofa domestica*) are increasingly used for biomedical and pharmaceutical studies due to the substantial analogies between porcine physiology and human physiology[24,25]. The porcine and human immune systems also share many similarities[25], including the expression and function of TLR8[26]. Thus, we next assessed T_{FH} cell differentiation in response to viable bacteria in pigs. Porcine CD172$^+$CD14$^+$ monocytes and CD172$^+$CD14$^-$ DCs were sorted from spleen samples of domestic pigs and were stimulated with live and dead bacteria. We used the thymidine-auxotrophic *E. coli* (EC) or a live attenuated strain of *Salmonella enterica* serovar Typhimurium (ST) (distributed under the trade name 'Salmoporc-STM') as a live *Salmonella* vaccine for pigs[27]. Salmoporc-STM bacteria are histidine–adenine auxotrophs, leading to severe growth attenuation. Porcine CD172$^+$CD14$^+$ monocytes and CD172$^+$CD14$^-$ DCs secreted large amounts of IL-12 in response to live EC and ST and the TLR8 agonist CL075 but not after stimulation with heat-killed ST (HKST) or HKEC (Fig. 6a,b). Secretion of IL-6 was induced similarly by live and dead EC and ST (Fig. 6a,b). Selective induction of IL-12 by live EC and ST was consistently observed (Fig. 6a–c), yet statistical testing did not reveal significant differences in this, due to limited sample size and high inter-experimental variation in cytokine production. Purified EC RNA also promoted increased secretion of IL-12p40 by porcine CD14$^+$ monocytes, as assessed by ELISA, a result that was not observed for ligands of TLR2 and TLR4 (Supplementary Fig. 4a). To determine whether the mechanisms of 'viability recognition' are conserved between human APCs and porcine APCs, we used RNA-mediated interference to silence the expression of the gene encoding TLR8 in porcine CD14$^+$ monocytes. Knockdown of *TLR8* abolished the expression of IL-12p40 in response to live ST, whereas the production of IL-6, which is induced independently of bacterial viability, was unaffected (Fig. 6c). We next assessed the effect of bacterial viability on porcine T_{FH} cell differentiation. Pig splenocytes (populations that included APCs and CD4$^+$ T cells) were stimulated for 1 h with varying doses of ST or HKST, followed by the addition of antibiotics

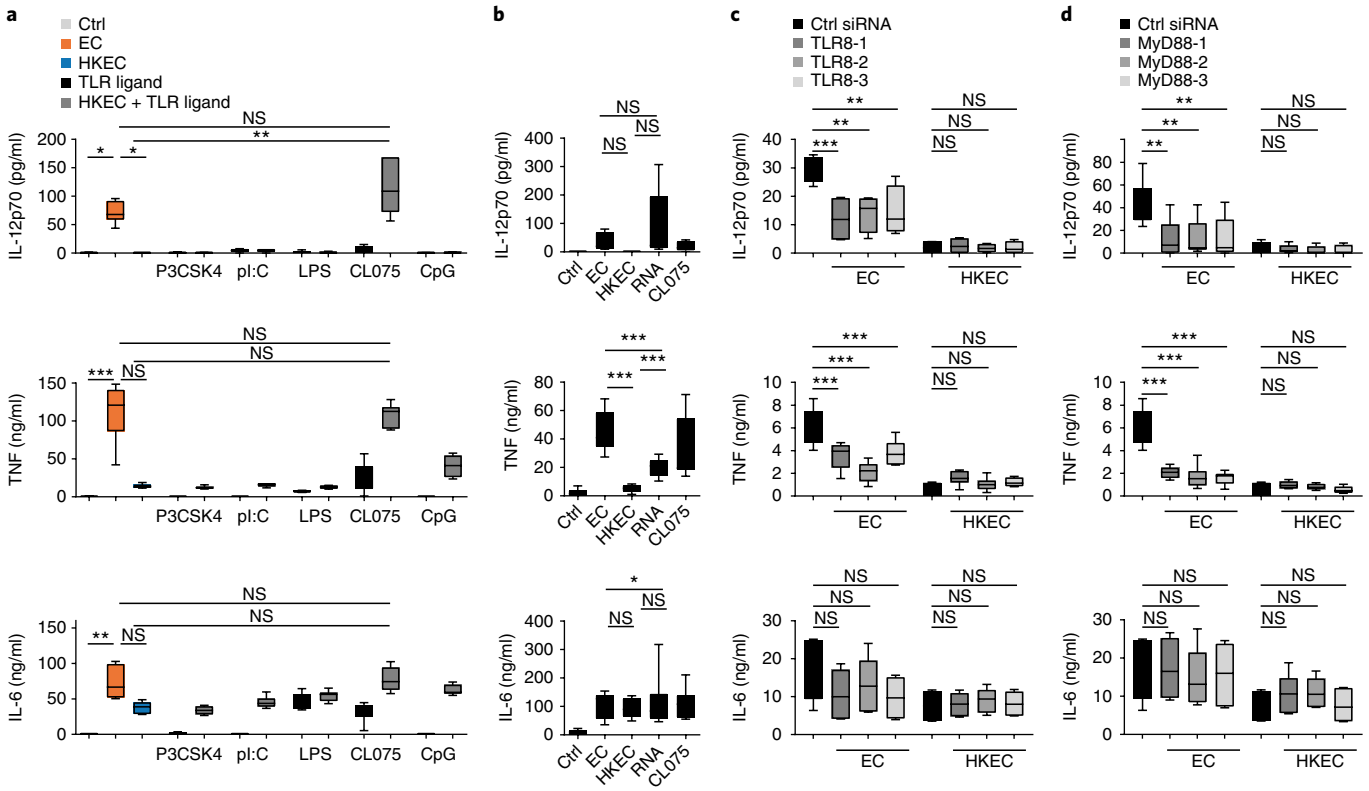

Fig. 4 | APCs sense live bacteria via TLR8. a, ELISA of IL-12p70 (top), TNF (middle) and IL-6 (bottom) in supernatants of monocytes ($n = 3$ donors) left untreated (Ctrl) or exposed to EC or HKEC or the TLR2 ligand Pam_3CSK_4 (P3CSK4), the TLR3 ligand poly(I:C) (pI:C), the TLR7 and TLR8 ligand CL075 or the TLR9 ligand CpG (horizontal axis) alone or exposed to HKEC supplemented with those TLR ligands (key). **b**, ELISA of cytokines as in **a** in supernatants of monocytes ($n = 4$ donors) left unstimulated (Ctrl) or stimulated with EC, HKEC, bacterial RNA (RNA) or CL075 (horizontal axis). **c**,**d**, ELISA of cytokines as in **a** in supernatants of human monocytes ($n = 3$ donors) treated with control siRNA with a scrambled sequence (Ctrl siRNA) or one of three siRNAs (-1, -2, -3; key) directed against TLR8 (**c**) or MyD88 (**d**) and stimulated with EC or HKEC (below plot). $^{**}P < 0.01$ and $^{***}P < 0.001$ (one-way ANOVA (**a**,**b**) or two-way ANOVA (**c**,**d**) with post-hoc correction for multiple comparisons). Data are representative of three experiments (**a**,**c**,**d**) or four experiments (**b**) (error bars, maximum and minimum).

to prevent residual bacterial growth, plus concanavalin A to induce polyclonal T cell proliferation. We observed a dose-dependent increase in the frequency of $CD4^+IL\text{-}21^+BCL\text{-}6^+$ T_{FH} cell–like cells in response to ST, compared with the frequency of such cells in response to stimulation with HKST (Fig. 6d,e). Next we compared the ability of soluble PAMPs to induce a T_{FH} cell phenotype in pig splenocytes in vitro. The TLR8 agonists bacterial RNA and CL075 induced $CD4^+IL21^+BCL\text{-}6^+$ T cells, but the TLR4 agonist LPS did not (Fig. 6f). Thus, recognition of bacterial viability via TLR8 constituted a critical stimulus of porcine T_{FH} cell differentiation.

Bacterial viability promotes T_{FH} cell differentiation in vivo. To directly assess the role of the detection of bacterial viability by the innate immune system in T_{FH} cell responses in vivo, we vaccinated domestic pigs with live attenuated ST (Salmoporc-STM), an equivalent dose of HKST or solvent (saline; as a control). The frequency of $CD4^+IL\text{-}21^+BCL\text{-}6^+$ T_{FH} cell–like cells was greater in the draining lymph nodes (dorsal superficial cervical nodes) and spleen of pigs immunized with Salmoporc-STM than in that of pigs immunized with HKST or saline (Fig. 7a,b) Other markers of effector T cell differentiation, including T-bet and FoxP3, were similarly altered in T cells from the ST-vaccinated or HKST-vaccinated groups (Supplementary Fig. 4b–e). We observed an increased number of $PAX5^+$ B cell follicles in the spleen of ST-vaccinated pigs relative to the number of such follicles in the spleen of saline-treated pigs, a result that was not observed for the HKST-vaccinated group compared with the saline-treated group (Fig. 7c,d), although the difference between the ST-vaccinated group and the HKST-vaccinated group did not reach statistical significance. B cell follicles in the spleen of ST-vaccinated pigs showed considerable enrichment for $Ki67^+PAX5^+$ B cells (Fig. 7e and Supplementary Fig. 5a), indicative of active germinal centers, but B cell follicles were negative for BCL2 (Supplementary Fig. 5b), which ruled out the possibility of malignant transformation. We also found an increased frequency of antibody-forming cells and plasma cells, which can be further separated into $CD3^-CD8^-SLAII^+IgM^+CD2^+CD21^-$ effector and $CD3^-CD8^-SLAII^+IgM^+CD2^-CD21^-$ resting antibody-forming cells and plasma cells[28], in ST-vaccinated pigs relative to the number of such cells in HKST-vaccinated pigs (Fig. 7f). Notably, higher levels of *Salmonella*-binding serum IgG were detected after vaccination with live ST than after vaccination with HKST (Fig. 7g), which demonstrated enhanced humoral immunity in response to the live vaccine. These results indicated that the recognition of bacterial viability was an essential driver of vaccine-induced T_{FH} cell and antibody responses in vivo.

A *TLR8* polymorphism is associated with vaccine protection in humans. Several functional polymorphisms in *TLR8* in humans have been described[29,30]. The *TLR8* single-nucleotide polymorphism (SNP) TLR8-A1G (rs3764880; called 'TLR8-G' here) alters the start codon ATG into a GTG triplet[29], which shifts the signal peptide by three amino acids, with a second in-frame ATG (M4) being used as an alternative start codon. According to in silico modeling predictions based on the published crystal structure of TLR8[31],

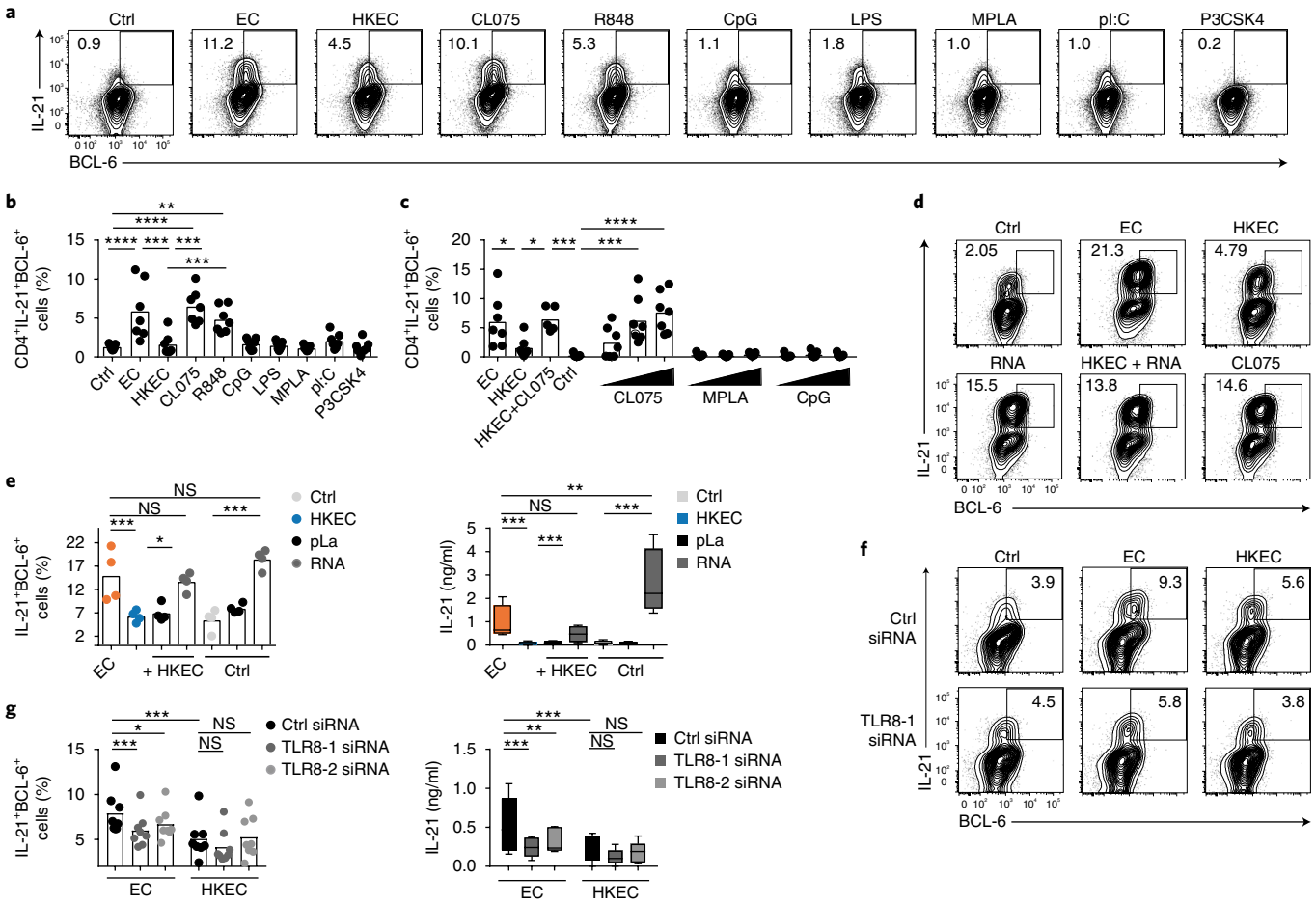

Fig. 5 | TLR8 senses bacterial viability and drives T_{FH} cell differentiation. a, Flow-cytometry analysis of the expression of IL-21 and BCL-6 by CD4$^+$ T cells ($n=7$ donors) stimulated in the presence of supernatants of APCs previously left unstimulated (Ctrl) or stimulated with EC or HKEC or various TLR ligands (above plots). **b**, Frequency of IL-21$^+$BCL-6$^+$ cells in cultures as in **a** (horizontal axis). **c**, Frequency of IL-21$^+$BCL-6$^+$ T cells (assessed by flow cytometry) following co-culture with APCs (as in Fig. 1) left unstimulated (Ctrl) or stimulated with EC, HKEC or HKEC plus CL075 or with increasing concentrations (wedges) of CL075 (0.1, 0.5 or 1 μg/ml), MPLA (0.1, 0.5 or 1 μg/ml) or CpG (0.1, 1 or 2.5 μM) (horizontal axis) . **d**, Flow-cytometry analysis of the expression of IL-21 and BCL-6 by CD4$^+$ T cells stimulated by supernatants of APCs previous left unstimulated (Ctrl) or stimulated with EC, HKEC, bacterial RNA, HKEC plus bacterial RNA, or CL075 (above plots). **e**, Frequency of IL-21$^+$BCL-6$^+$ cells in cultures of CD4$^+$ T cells stimulated by supernatants of APCs previously left unstimulated (Ctrl) or stimulated with EC or HKEC (horizontal axis) and the polycationic polypeptide poly-L-arginine (pLa) or bacterial RNA (key) (left), and ELISA of IL-21 in supernatants of those cultures (right). **f**,**g**, Flow-cytometry analysis of the expression of IL-21 and BCL-6 by CD4$^+$ T cells stimulated by supernatants of APCs previously left unstimulated (Ctrl) or stimulated with EC or HKEC (above plots) and treated with control or TLR8-specific siRNA (left margin) (**f**), frequency of IL-21$^+$BCL-6$^+$ cells in cultures as in **f** (key) (**g**, left) and ELISA of IL-21 in supernatants of cultures as in **f** (key) (**g**, right). Each symbol (**b**,**c**,**e**,**g**) represents an individual donor ($n=7$ (**b**), $n=7$ (**c**), $n=4$ (**e**) or $n=8$ (**g**)). *$P<0.05$, **$P<0.01$, ***$P<0.001$ and ****$P<0.0001$ (one-way ANOVA (**b**,**c**) or two-way ANOVA (**e**,**g**) with post-hoc correction for multiple comparisons). Data are representative of seven experiments (**a**–**c**), four experiments (**d**,**e**) or eight experiments (**f**,**g**) (error bars (**e**,**g**, right), maximum and minimum).

the amino-acid truncation leads to significant structural alterations to the protein (Supplementary Fig. 6 and Supplementary Note 1). The increased disorder, free energy and increased flexibility of the protein encoded by TLR8-G (Supplementary Fig. 6) probably make the receptor better adapted to side-chain rearrangement and dimerization. The larger volume of clefts and cavities on the surface of the protein encoded by TLR8-G than on that encoded by TLR8-A (the protein encoded by *TLR8* without the SNP rs3764880) might increase its potential for ligand binding, whereas functional pockets and nests are slightly decreased (Supplementary Fig. 7). These models suggest altered receptor functionality, which might cause a gain of function for the receptor encoded by the TLR8-G variant. In line with those predictions, APCs from individuals expressing the TLR8-G variant showed a slightly enhanced release of IL-12 in response to stimulation of TLR8, but not in response to the TLR4 agonist LPS, relative to the response of APCs derived from carriers of TLR8-A (Supplementary Fig. 8a,b). We also studied HEK293T human embryonic kidney cells expressing a reporter gene to measure actvity of the transcription factor NF-κB. Such cells stably expressing the TLR8-G variant showed higher NF-κB-reporter activity in response to TLR8 ligands than that of their TLR8-A-expressing counterparts (Supplementary Fig. 8c), in support of the proposed gain-of-function phenotype of the TLR8-G variant.

Carriage of the TLR8-G allele has been associated with slower progression of infection with human immunodeficiency virus[29] and protection against pulmonary TB (PTB)[32]. Here we assessed distribution of the TLR8-G allelein 293 patients with confirmed TB and 165 of their healthy household contacts (control subjects; Supplementary Table 2). Significantly more control subjects (53.9%) than patients with TB (41.3%) were homo- or hemizygous carriers

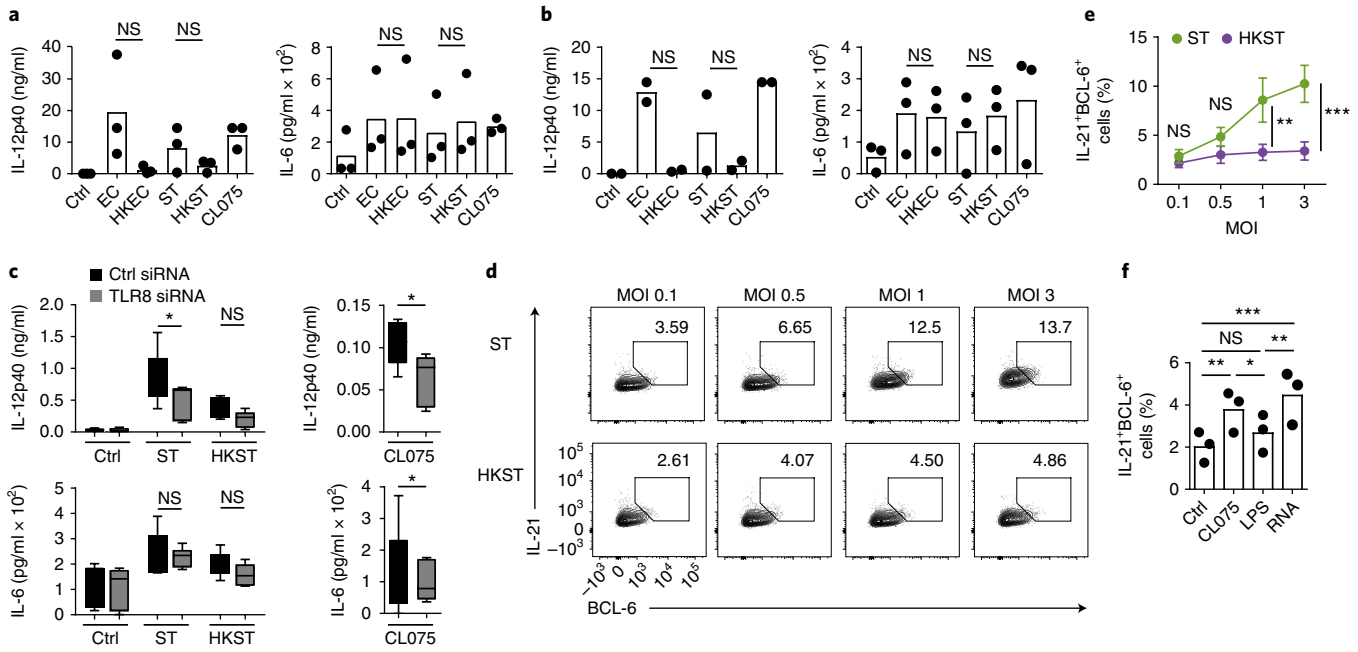

Fig. 6 | Detection of viable bacteria via TLR8 by porcine APCs promotes T_{FH} cell differentiation. a,**b**, Multiplex bead array of IL-12p40 (left) and IL-6 (right) in cultures of porcine CD14⁺CD172⁺ monocytes (**a**) or CD14⁻CD172⁺ DCs (**b**) sorted from spleen samples and stimulated with medium (Ctrl), EC, HKEC, ST, HKST or CL075 (horizontal axis). **c**, ELISA of IL-12p40 (top) and IL-6 (bottom) in supernatants of porcine splenic CD14⁺ monocytes ($n=3$ pigs) treated with control siRNA or siRNA directed against porcine TLR8 (key) and stimulated with medium (Ctrl), ST, HKST or CL075 (horizontal axis). **d**, Flow-cytometry analysis of the expression of IL-21 and BCL-6 by CD4⁺ T cells among porcine splenocytes stimulated for 4 d with concanavalin A in the presence of increasing doses (above plots) of ST (top) or HKST (bottom) (left margin). **e**, Frequency of IL-21⁺BCL-6⁺ cells in cultures as in **d** ($n=3$ pigs). **f**, Frequency of IL-21⁺BCL-6⁺ cells among CD4⁺ T cells in cultures of porcine splenocytes stimulated for 4 d with medium (Ctrl), CL075, LPS or bacterial RNA (horizontal axis) in the presence of concanavalin A. Each symbol (**a**,**b**,**f**) represents an individual pig ($n=3$ (IL-6 (**a**,**b**)) or 2 (IL-12p40 (**b**)) (**a**,**b**), or $n=3$ (**f**)). $^{*}P<0.05$, $^{**}P<0.01$ and $^{***}P<0.001$ (one-way ANOVA (**a**,**b**,**f**) or two-way ANOVA (**c**, **e**) with post-hoc correction for multiple comparisons). Data are representative of three experiments (error bars, maximum and minimum (**c**) or mean ± s.e.m. (**e**)).

of TLR8-G (Fig. 8a and Supplementary Table 3). The TLR8-A allele was associated with significantly increased odds for infection with *M. tuberculosis* (odds ratio = 1.94 [95% confidence interval, 1.194–3.156]; $P=0.007$), and similar results were obtained for the subgroup of patients with PTB (Fig. 8a and Supplementary Table 3), indicative of a protective effect of TLR8-G against PTB, as has been reported[32]. Further subgroup analysis revealed that distribution of the *TLR8* allele was in fact significantly different only for subjects who had previously received the live BCG vaccine against TB ($P=0.002$), whereas its distribution was not significantly different for unvaccinated subjects ($P=0.754$) (Fig. 8a and Supplementary Table 4). In this study, vaccination with BCG was associated with significant risk protection in carriers of the TLR8-G allele (odds ratio = 0.280 [95% confidence interval, 0.105–0.742]) but not in carriers of the TLR8-A allele (Fig. 8b and Supplementary Table 4). These epidemiological results indicated that TLR8-G was associated with improved BCG vaccine–mediated protection without affecting susceptibility to PTB itself, and they linked the function of TLR8 to protective immunity in response to a live bacterial vaccine in a large human cohort.

Discussion

Here we have identified the recognition of microbial viability as a hard-wired, conserved immune checkpoint that regulates innate and adaptive immunity. We have described TLR8 as a receptor for vita-PAMPs in humans and pigs. Activation of TLR8 by bacterial RNA served to distinguish live bacteria from dead bacteria and controlled downstream cytokine and T_{FH} cell responses. Accordingly, we found that carriage of a hypermorphic *TLR8* polymorphism was associated with improved vaccine-induced protection. Immunization with live attenuated bacteria induced T_{FH} cell differentiation and antibody responses in pigs, but immunization with the killed version of the same vaccine did not. Hence, we have provided experimental and epidemiological evidence to support the proposal of a critical role for viability recognition and TLR8 signals in the immune response to live attenuated vaccines.

Despite the need for improved vaccine adjuvants, knowledge about the innate signals that control the differentiation of human T_{FH} cells is scarce. Heat-killed bacteria and LPS have been reported to induce T_{FH} cell differentiation mediated by human monocyte-derived DCs[33]. The apparent discrepancy with our findings that LPS and dead bacteria were poor stimulators of T_{FH} cell responses in primary monocytes and DCs can probably be explained by the fact that monocyte-derived DCs readily produce IL-12 due to differentiation in IL-4-containing medium[34], whereas we used primary cells not grown in IL-4-containing medium. Published mouse studies have suggested a T_{FH} cell–promoting effect of TLR agonists such as CpG DNA[35,36]. In human APCs, most TLR ligands are weak inducers of T_{FH} cell differentiation, relative to stimulation with viable bacteria or TLR8 agonists. However, the repertoire and function of innate immune receptors of mouse APCs differ from those of human APCs. For example, mouse TLR8 is unresponsive to single-stranded RNA[37]. The cytokine requirement for the differentiation of human T_{FH} cells is also different from that for mouse T_{FH} cells[9,18,20,38]. Thus, while innate sensing of bacterial RNA is a conserved trigger for T_{FH} cell and antibody responses in both species[7,39], the different signaling pathways have to be taken into account in the translation of findings from mouse vaccine studies to human vaccine studies. Interestingly, TLR8 agonists have been shown to possess unique adjuvant activity in other species, including non-human primates[40,41]. Here we studied

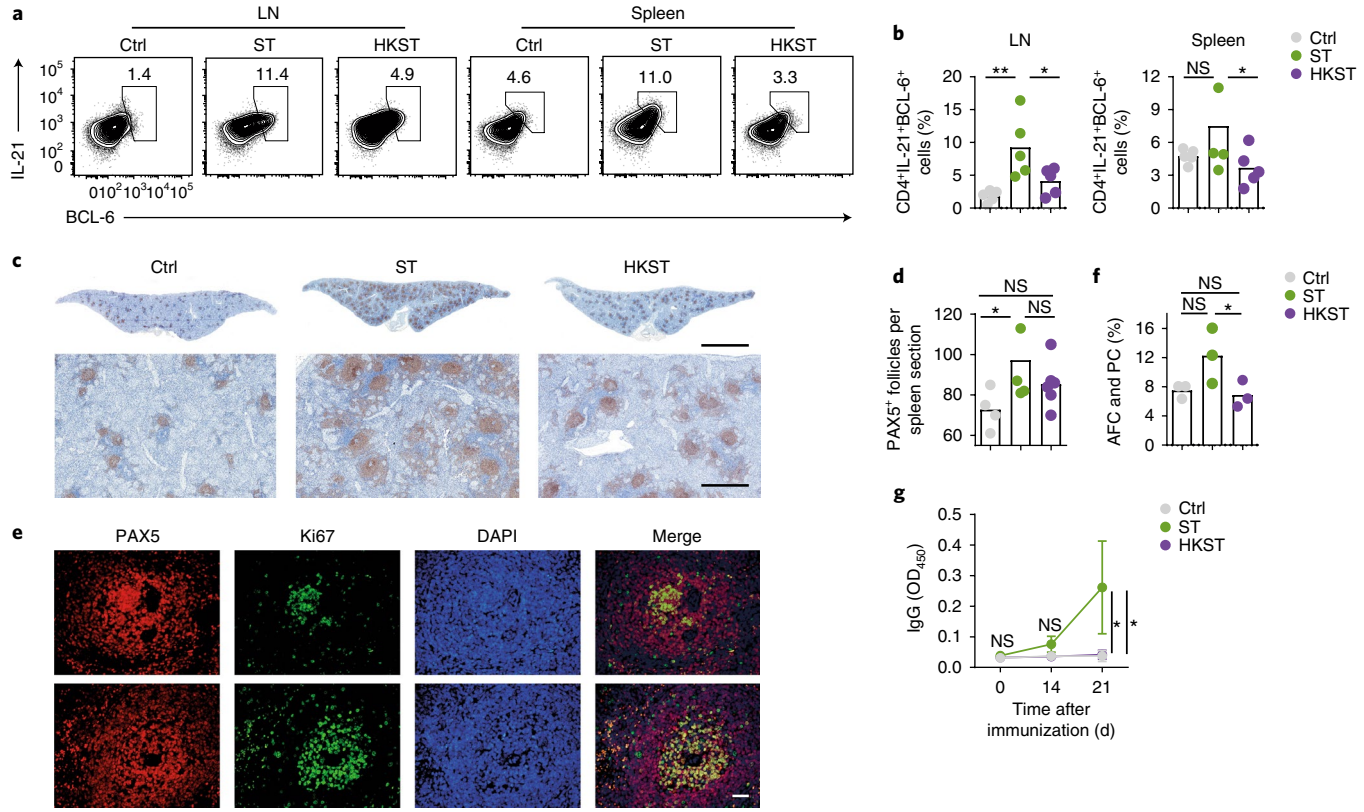

Fig. 7 | A live attenuated vaccine promotes T_{FH} cell differentiation in swine. a, Flow-cytometry analysis of the expression of IL-21 and BCL-6 by $CD4^+$ T cells from the draining lymph nodes (LN) or spleen of 5-week-old domestic piglets on day 30 after subcutaneous immunization with saline (Ctrl), ST or HKST (above plots). **b**, Frequency of $IL\text{-}21^+BCL\text{-}6^+$ cells in lymph nodes or spleen (above plots) of pigs as in **a** (key). **c**, Microscopy of paraffin-embedded sections of spleen tissues from pigs as in **a** (above images), stained for the transcription factor PAX5. Scale bars, 5 mm (top) or 500 μm (bottom). **d**, Morphometric quantification of $PAX5^+$ follicles in spleen sections of pigs as in **c** (key). **e**, Microscopy of co-immunofluorescence staining of PAX5 (red) and Ki67 (green) on sections of spleen from pigs vaccinated with ST; cell nuclei were stained with the DNA-binding dye DAPI (blue). Each row shows a follicle from a separate pig. Scale bar, 50 μm. **f**, Frequency of antibody-forming cells (AFC) and plasma cells (PC) among lymphocytes in spleen samples of pigs as in **c** (key), assessed by flow cytometry. **g**, ELISA of anti-*Salmonella* IgG in serum samples obtained from pigs as in **c** (key) before vaccination (day 0) and on day 14 and 21 after vaccination (horizontal axis), presented as the optical density at 450 nm (OD_{450}). Each symbol (**b**,**d**,**f**) represents an individual pig ($n=5$ per group (**b**) or ($n=3$ per group (**f**)). $^*P<0.05$ and $^{**}P<0.01$ (one-way ANOVA (**b**,**d**) or two-way ANOVA (**g**) with post-hoc correction for multiple comparisons). Data are representative of one experiment with various numbers of pigs in each panel (as indicated in legend above; error bars (**g**), mean ± s.e.m.).

vaccine responses to live attenuated bacteria in domestic pigs, given the closer resemblance of their physiology to human physiology than that of laboratory mice in terms of size, life span, organ anatomy, diet, circadian rhythm and immunity[24,42]. More importantly, domestic farm animals represent critical vaccine populations. Efficient vaccines would help to lower antibiotic consumption and thereby reduce the development of antibiotic resistance[43]. The emergence of zoonotic infections has added to the need for efficacious veterinary vaccines. Our study has provided the first evidence, to our knowledge, of T_{FH} cell–like cells in pigs and has described the induction of such cells after the recognition of live attenuated bacteria. While additional studies are needed for full characterization of the generation of protective immunity in pigs, our study contributes new insights into the mechanisms of live attenuated vaccines and highlights swine as a valuable species for research into T_{FH} cells and vaccines.

Our epidemiological study linked a hypermorphic *TLR8* polymorphism to enhanced vaccine-induced protection. The epidemiological data support our experimental observations and might also help to explain the variable efficacy of vaccination with BCG[44]. In contrast to several SNPs, primary TLR8 deficiency has not been reported so far. Patients with genetic defects in the TLR adaptors MyD88 or IRAK4 suffer from recurrent bacterial infections[45,46], but the frequency of T_{FH} cells in people with these rare gene defects has not been investigated. Individuals with loss-of-function mutations in the gene encoding the IL-12 receptor (*IL12RB1*) have a lower number of circulating T_{FH} cells and reduced GC formation in lymph nodes[38]. Other studies have reported a less-pronounced reduction in T_{FH} cells; however, these studies included fewer subjects[47,48]. Notably, antibody levels are largely normal in *IL12RB1*-deficient persons; however, the avidity of their serum IgG for some antigens is lower[38]. Better characterization of human immune responses in patients with primary immunodeficiencies might facilitate the identification of non-redundant pathways for efficient T_{FH} cell responses.

Given the broad functionality of high-affinity antibody responses, it has been proposed that microbial stimulation, or PAMPs in general, induce the formation of T_{FH} cells[9]. However, while high-affinity antibodies are indeed a versatile mechanism of defense against most pathogens, uncontrolled activation of T_{FH} cells can cause debilitating diseases and must be tightly controlled[17,49]. Antimicrobial immune responses are therefore tightly scaled to the level of the microbial threat[6]. The recognition of bacterial RNA as a molecular signature of microbial viability and increased microbial threat[7] constitutes a critical trigger for T_{FH} cell differentiation. This provides an efficient checkpoint for T_{FH} cell responses without limiting the versatility of high-affinity antibodies in antimicrobial host defense. Although live vaccines are diverse and activate multiple pathways, we propose

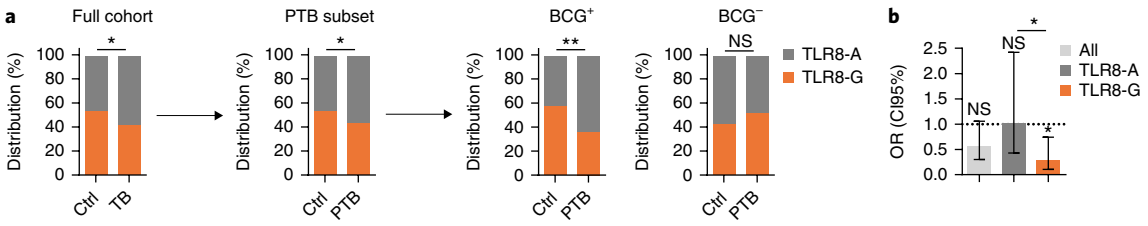

Fig. 8 | Association of a *TLR8* SNP with BCG-induced immunity. a, Distribution of the TLR8-A and TLR8-G alleles (key) in the entire cohort of subjects ($n=458$: $n=293$ subjects with confirmed TB and $n=165$ household contacts (Ctrl); horizontal axis) (far left) and in a subset of subjects ($n=345$: $n=180$ subjects with confirmed PTB and $n=165$ household contacts (Ctrl); horizontal axis) (middle left), and distribution of those alleles in BCG-vaccinated (BCG^+) and unvaccinated (BCG^-) subjects (above plots) with confirmed PTB and their household contacts (horizontal axis) (right; one subject excluded due to unclear vaccination status). **b**, Odds ratio (adjusted for sex, age and body mass index) for PTB in BCG-vaccinated versus unvaccinated subjects, calculated for the whole study population (All) and separately for each *TLR8* genotype (key), presented as odds ratio (OR) (bars) and 95% confidence interval (CI95%) (error bars). $^*P<0.05$ and $^{**}P<0.01$, TLR8-A versus TLR8-G (Wald's test).

the sensing of microbial viability by the innate immune system as a unifying motif of live attenuated vaccines. Thus, the identification of TLR8 as a critical sensor of vita-PAMPs will provide opportunities for the development of T_{FH} cell–targeted vaccine adjuvants, which are sorely needed to improve existing and future inanimate subunit vaccines directed against a broad range of infectious and non-infectious diseases.

Methods

Methods, including statements of data availability and any associated accession codes and references, are available at https://doi.org/10.1038/s41590-018-0068-4.

Received: 19 July 2016; Accepted: 15 February 2018;
Published online: 19 March 2018

References

1. Barquet, N. & Domingo, P. Smallpox: the triumph over the most terrible of the ministers of death. *Ann. Intern. Med.* **127**, 635–642 (1997).
2. Plotkin, S. A. & Plotkin, S. L. The development of vaccines: how the past led to the future. *Nat. Rev. Microbiol.* **9**, 889–893 (2011).
3. Minor, P. D. Live attenuated vaccines: Historical successes and current challenges. *Virology* **479–480**, 379–392 (2015).
4. De Gregorio, E. & Rappuoli, R. From empiricism to rational design: a personal perspective of the evolution of vaccine development. *Nat. Rev. Immunol.* **14**, 505–514 (2014).
5. Rauh, L. W. & Schmidt, R. Measles immunization with killed virus vaccine. Serum antibody titers and experience with exposure to measles epidemic. *Am. J. Dis. Child.* **109**, 232–237 (1965).
6. Blander, J. M. & Sander, L. E. Beyond pattern recognition: five immune checkpoints for scaling the microbial threat. *Nat. Rev. Immunol.* **12**, 215–225 (2012).
7. Sander, L. E. et al. Detection of prokaryotic mRNA signifies microbial viability and promotes immunity. *Nature* **474**, 385–389 (2011).
8. Iwasaki, A. & Medzhitov, R. Control of adaptive immunity by the innate immune system. *Nat. Immunol.* **16**, 343–353 (2015).
9. Crotty, S. T follicular helper cell differentiation, function, and roles in disease. *Immunity* **41**, 529–542 (2014).
10. Vinuesa, C. G., Linterman, M. A., Yu, D. & MacLennan, I. C. Follicular helper T cells. *Annu. Rev. Immunol.* **34**, 335–368 (2016).
11. Johnston, R. J. et al. Bcl6 and Blimp-1 are reciprocal and antagonistic regulators of T follicular helper cell differentiation. *Science* **325**, 1006–1010 (2009).
12. Nurieva, R. I. et al. Bcl6 mediates the development of T follicular helper cells. *Science* **325**, 1001–1005 (2009).
13. Linterman, M. A. et al. IL-21 acts directly on B cells to regulate Bcl-6 expression and germinal center responses. *J. Exp. Med.* **207**, 353–363 (2010).
14. Weber, J. P. et al. ICOS maintains the T follicular helper cell phenotype by down-regulating Kruppel-like factor 2. *J. Exp. Med.* **212**, 217–233 (2015).
15. Breitfeld, D. et al. Follicular B helper T cells express CXC chemokine receptor 5, localize to B cell follicles, and support immunoglobulin production. *J. Exp. Med.* **192**, 1545–1552 (2000).
16. Schaerli, P. et al. CXC chemokine receptor 5 expression defines follicular homing T cells with B cell helper function. *J. Exp. Med.* **192**, 1553–1562 (2000).
17. Ueno, H., Banchereau, J. & Vinuesa, C. G. Pathophysiology of T follicular helper cells in humans and mice. *Nat. Immunol.* **16**, 142–152 (2015).
18. Cucak, H., Yrlid, U., Reizis, B., Kalinke, U. & Johansson-Lindbom, B. Type I interferon signaling in dendritic cells stimulates the development of lymph-node-resident T follicular helper cells. *Immunity* **31**, 491–501 (2009).
19. Batten, M. et al. IL-27 supports germinal center function by enhancing IL-21 production and the function of T follicular helper cells. *J. Exp. Med.* **207**, 2895–2906 (2010).
20. Schmitt, N. et al. The cytokine TGF-β co-opts signaling via STAT3-STAT4 to promote the differentiation of human TFH cells. *Nat. Immunol.* **15**, 856–865 (2014).
21. Jacquemin, C. et al. OX40 ligand contributes to human lupus pathogenesis by promoting T follicular helper response. *Immunity* **42**, 1159–1170 (2015).
22. Eigenbrod, T., Pelka, K., Latz, E., Kreikemeyer, B. & Dalpke, A. H. TLR8 senses bacterial RNA in human monocytes and plays a nonredundant role for recognition of *Streptococcus pyogenes*. *J. Immunol.* **195**, 1092–1099 (2015).
23. Bergstrom, B. et al. TLR8 senses *Staphylococcus aureus* RNA in human primary monocytes and macrophages and induces IFN-β production via a TAK1-IKKβ-IRF5 signaling pathway. *J. Immunol.* **195**, 1100–1111 (2015).
24. Meurens, F., Summerfield, A., Nauwynck, H., Saif, L. & Gerdts, V. The pig: a model for human infectious diseases. *Trends Microbiol.* **20**, 50–57 (2012).
25. Mair, K. H. et al. The porcine innate immune system: an update. *Dev. Comp. Immunol.* **45**, 321–343 (2014).
26. Zhu, J., Lai, K., Brownile, R., Babiuk, L. A. & Mutwiri, G. K. Porcine TLR8 and TLR7 are both activated by a selective TLR7 ligand, imiquimod. *Mol. Immunol.* **45**, 3238–3243 (2008).
27. Springer S., Lindner T., Steinbach G., Selbitz H. J. Investigation of the efficacy of a genetically-stabile live *Salmonella typhimurium* vaccine for use in swine. *Berl. Munch. Tierarztl. Wochenschr.* **114**,342–345 (2001).
28. Sinkora, M., Stepanova, K. & Sinkorova, J. Different anti-CD21 antibodies can be used to discriminate developmentally and functionally different subsets of B lymphocytes in circulation of pigs. *Dev. Comp. Immunol.* **39**, 409–418 (2013).
29. Oh, D. Y. et al. A functional toll-like receptor 8 variant is associated with HIV disease restriction. *J. Infect. Dis.* **198**, 701–709 (2008).
30. Wang, C. H. et al. TLR7 and TLR8 gene variations and susceptibility to hepatitis C virus infection. *PLoS One* **6**, e26235 (2011).
31. Tanji, H., Ohto, U., Shibata, T., Miyake, K. & Shimizu, T. Structural reorganization of the Toll-like receptor 8 dimer induced by agonistic ligands. *Science* **339**, 1426–1429 (2013).
32. Davila, S. et al. Genetic association and expression studies indicate a role of toll-like receptor 8 in pulmonary tuberculosis. *PLoS Genet.* **4**, e1000218 (2008).
33. Schmitt, N. et al. Human dendritic cells induce the differentiation of interleukin-21-producing T follicular helper-like cells through interleukin-12. *Immunity* **31**, 158–169 (2009).
34. Hochrein, H. et al. Interleukin (IL)-4 is a major regulatory cytokine governing bioactive IL-12 production by mouse and human dendritic cells. *J. Exp. Med.* **192**, 823–833 (2000).
35. Jones, S. C., Brahmakshatriya, V., Huston, G., Dibble, J. & Swain, S. L. TLR-activated dendritic cells enhance the response of aged naive CD4 T cells via an IL-6-dependent mechanism. *J. Immunol.* **185**, 6783–6794 (2010).
36. Chakarov, S. & Fazilleau, N. Monocyte-derived dendritic cells promote T follicular helper cell differentiation. *EMBO Mol. Med.* **6**, 590–603 (2014).

37. Heil, F. et al. Species-specific recognition of single-stranded RNA via toll-like receptor 7 and 8. *Science* **303**, 1526–1529 (2004).
38. Schmitt, N. et al. IL-12 receptor beta1 deficiency alters in vivo T follicular helper cell response in humans. *Blood* **121**, 3375–3385 (2013).
39. Barbet, G. et al. Sensing microbial viability through bacterial RNA augments T follicular helper cell and antibody responses. *Immunity* (in the press).
40. Dowling, D. J. et al. TLR7/8 adjuvant overcomes newborn hyporesponsiveness to pneumococcal conjugate vaccine at birth. *JCI Insight* **2**, e91020 (2017).
41. Dowling, D. J. et al. Toll-like receptor 8 agonist nanoparticles mimic immunomodulating effects of the live BCG vaccine and enhance neonatal innate and adaptive immune responses. *J. Allergy Clin. Immunol.* **140**, 1339–1350 (2017).
42. Fairbairn, L., Kapetanovic, R., Sester, D. P. & Hume, D. A. The mononuclear phagocyte system of the pig as a model for understanding human innate immunity and disease. *J. Leukoc. Biol.* **89**, 855–871 (2011).
43. Landers, T. F., Cohen, B., Wittum, T. E. & Larson, E. L. A review of antibiotic use in food animals: perspective, policy, and potential. *Public Health Rep.* **127**, 4–22 (2012).
44. Colditz, G. A. et al. Efficacy of BCG vaccine in the prevention of tuberculosis. Meta-analysis of the published literature. *J. Am. Med. Assoc.* **271**, 698–702 (1994).
45. de Beaucoudrey, L. et al. Revisiting human IL-12Rβ deficiency: a survey of 141 patients from 30 countries. *Medicine (Baltimore)* **89**, 381–402 (2010).
46. Picard, C. et al. Clinical features and outcome of patients with IRAK-4 and MyD88 deficiency. *Medicine (Baltimore)* **89**, 403–425 (2010).
47. Ma, C. S. et al. Functional STAT3 deficiency compromises the generation of human T follicular helper cells. *Blood* **119**, 3997–4008 (2012).
48. Ma, C. S. et al. Monogenic mutations differentially affect the quantity and quality of T follicular helper cells in patients with human primary immunodeficiencies. *J. Allergy Clin. Immunol.* **136**, 993–1006 (2015).
49. Rao, D. A. et al. Pathologically expanded peripheral T helper cell subset drives B cells in rheumatoid arthritis. *Nature* **542**, 110–114 (2017).

Acknowledgements

We thank D. Kunkel, S. Warth and A. Linke for technical advice; the flow cytometry facility of the Berlin Brandenburg Center for Regenerative Therapies (BCRT) of the Charité Berlin; S. Springer and IDT Biologika for assistance in planning the animal studies and for the Salmoporc STM vaccine; and R. Nifosí for critical review of the modelling analysis. Supported by the German Research Council (DFG grant SA1940-2/1 and SFB-TR84 TP C8 to L.E.S.; SFB-TR84 TP B1 to N.S.; SFB-TR-84 TP A1/A5 to B.O.; SFB-TR84 TP Z1b to A.D.G.; DFG-GRK 1673 project to R.R.S.; and DFG-GRK 2046, TP4 to S.H.), the European Research Council and the Federal Ministry of Education and Research (FP-7 ERA-NET / Infect-ERA consortium "HaploINFECT" / BMBF 031A402A to L.E.S., VIP + VALNEMCYS project and InfectControl 2020, consortium Art4Fun to S.H.), the European Society of Clinical Microbiology and Infectious Diseases (ESCMID research grant to L.E.S.), the Jürgen Manchot Foundation (Doctoral Research Fellowship to P.G., E.T.H. and S.M.V.), the Netherlands Nutrigenomics Center, Wageningen University, The Netherlands (to M.M. and M.B.), the Fritz Thyssen Foundation (research grant to A.H.), The Danish National Research Foundation (grant no. DNRF108 to) to Research Centre for Vitamins and Vaccines (CVIVA) supporting K.J.J., and The Novo Nordisk Foundation supporting the pig vaccination experiments at Technical University of Denmark, Federal Ministry of Education and Research.

Author contributions

M.U. and J.G. designed and performed experiments; S.B. analyzed clinical data and performed experiments; K.J.J., C.S.B., G.J. and L.E.S. planned and performed animal studies; P.G., F.E., S.M.V., S.T., K.D., L.B. and E.T.H. performed experiments; M.U., J.G., P.G., F.E., S.M.V., K.D., B.O., F.K., A.D.G., A.H., S.H., M.M., N.S. and L.E.S. analyzed data and wrote the manuscript; S.S. performed structure prediction analysis; N.D., S.G., M.L.C. and R.R.S. designed and performed clinical studies; A.S. and U.B. provided samples and conceptual input; M.V.B. performed transcriptome analysis; and L.E.S. conceived of the study and designed experiments.

Competing interests

The authors declare no competing interests.

Additional information

Supplementary information is available for this paper at https://doi.org/10.1038/s41590-018-0068-4.

Reprints and permissions information is available at www.nature.com/reprints.

Correspondence and requests for materials should be addressed to L.E.S.

Publisher's note: Springer Nature remains neutral with regard to jurisdictional claims in published maps and institutional affiliations.

Methods

Cell isolation and culture. Human monocytes, T cells and B cells used in this study were either freshly isolated from peripheral venous blood of healthy volunteers or from buffy coats obtained from the German Red Cross Blood Transfusion Service, Berlin, Germany. Permission for experiments with human primary cells was obtained from Charité ethic committee (Charité – Universitätsmedizin Berlin, Germany). Peripheral blood mononuclear cells (PBMCs) were isolated by density gradient centrifugation over Histopaque-1077 (Sigma-Aldrich). $CD14^+CD16^-$ monocytes were purified by negative selection via immunomagnetic separation using EasySep monocyte isolation kits with CD16 depletion (StemCell Technologies) according to the manufacturer's instructions. Isolated monocytes were cultured at a density of 1×10^6 cells per ml in RPMI1640 supplemented with 10% FCS, 1% glutamine, 1% HEPES buffer and 1% non-essential amino acids (all from Sigma-Aldrich). T cells were cultured in RPMI1640 supplemented with 10% human serum (from the same T cell donor), 1% glutamine, 1% HEPES buffer and 1% non-essential amino acids; some T cell conditions were supplemented with 2.5 ng/ml of TGF-β (eBioscience). All cells were grown at 37 °C, 5% CO_2 in a humidified incubator.

Untreated human $CD1^+$ mDCs were purified by negative selection via immunomagnetic bead separation (Miltenyi Biotec) following the manufacturer's instructions.

Naive $CD4^+$ T cells were purified by immunomagnetic separation using negative selection (MagniSort Human CD4 Naive T cell Enrichment Kit, eBioscience). Total $CD4^+$ T cells (used in Figs. 3a,b,d and 4f,g and Supplementary Fig. 3) were isolated by magnetic separation using negative selection (MagniSort Human CD4 T cell Enrichment Kit, eBioscience).

Untreated naive human B cells were isolated by immunomagnetic bead separation (Miltenyi Biotec) following the manufacturer's instructions.

Cell purity was routinely checked by flow cytometry and only cells with a purity of > 85% (monocytes) or > 95% (T cells and B cells) were used for subsequent experiments.

Bacteria and infection. *Escherichia coli* K12, strain DH5α, thymidine auxotrophs (*thyA*$^-$) were selected as previously described[4]. Auxotrophy was confirmed by inoculation and overnight culture of single colonies in LB medium. *ThyA*$^-$ *E. coli* (EC) grew only in the presence of thymidine and were resistant to trimethoprim. For phagocytosis experiments, EC were grown to mid-log phase and were washed twice in phosphate-buffered saline (PBS) to remove thymidine and LB salts before addition to cells. For heat killing, EC were grown to log phase, were washed and re-suspended in PBS at an optical density at 600 nm (OD_{600}) of 0.6, and were subsequently incubated at 60 °C for 90 min. Heat-killed *thyA*$^-$ *E. coli* (HKEC) were used immediately after killing or were stored at −80 °C for up to 3 months. Efficient killing was confirmed by overnight plating on thymidine-trimethoprim–supplemented LB-agar plates. Alternatively, *Bacillus subtilis* strain 168 was used for analogous infection experiments. For heat killing, *B. subtilis* were grown to mid-log phase, were washed and re-suspended in PBS at an optical density at 600 nm (OD_{600}) of 0.6, and were subsequently incubated at 95 °C for 30 min. Efficient killing was confirmed by overnight plating on LB-agar plates. For heat killing, *S. enterica* serovar Typhimurium were grown to mid-log phase, were washed and re-suspended in PBS at an optical density at 600 nm (OD_{600}) of 0.6, and were subsequently incubated at 95 °C for 30 min. Efficient killing was confirmed by overnight plating on LB-agar plates. Infection of human monocyte was performed at the multiplicity of infection (MOI) indicated in the figure or text.

BCG were grown in Middlebrook 7H9 medium supplemented with 0.05% Tween 80. For phagocytosis experiments, BCG were grown to mid-log phase, were washed once in phosphate buffered saline (PBS) and were resuspended in complete cell culture media via repeated tuberculin type needle passages (10×). For heat killing, BCG were grown to log phase and were incubated at 60 °C for 90 min. Heat-killed BCG (HKBCG) were used immediately after killing. Efficient killing was confirmed by 96 h of inoculation in competent media.

Co-culture assay. For monocyte–T cell co-cultures, monocytes were cultured as described above and were stimulated as indicated (for example, EC, HKEC MOI 1–25) in antibiotics-free medium. After 1.5 h, penicillin-streptomycin (1%) was added, together with autologous naive $CD4^+$ T cells at a monocyte/T cell ratio of 2:1, plus staphylococcal enterotoxin B (SEB, Sigma) at a concentration of 1.0 μg/ml. After 5 d of co-culture T cells were harvested and washed, then were restimulated with phorbol-12-myristat-13-acetat (PMA, 50ng/ml) and ionomycin (1 μg/ml, both obtained from Sigma), stained and analyzed by flow cytometry.

For T cell–B cell co-cultures, T cells were differentiated by co-culture with autologous monocytes for 6 d as described in the previous subsection. $CXCR5^+ICOS^+PD\text{-}1^{hi}$ T cells were sorted by flow cytometry (BD FACSAria II) and were added to naive autologous B cells at a T cell/B cell ratio of 1:2 in the presence of SEB (1μg/ml). After 12 d of co-culture, B cells and T cells were harvested and analyzed by flow cytometry. For analysis of plasmablast differentiation, sorted T_{FH} cells ($CD19^-CD4^+CD45RA^-CXCR5^+$) or naive T cells ($CD19^-CD4^+CD45RA^+$) were co-cultured with memory B cells at a ratio of 1:1 in the presence of 4 ng/ml SEB for 7 d.

Antibodies and reagents. Antibodies to the following antigens were used for flow cytometry: CD3 (UCHT1, cat.: 300415), CD4 (OKT4, cat.: 317424), IFN-γ (4 S.B3, cat.: 502528), IL-17 (BL168, cat.: 512306), CXCR5 (J252D4, cat.: 356904), PD-1 (EH12.2H7, cat.: 329922), ICOS (C398.4 A, cat.: 313510), CD19 (HIB19, cat.: 302228 or SJ25C1, cat.: 363022), CD20 (2H7, cat.: 302324), CD27 (O323, cat.: 302810), CD38 (HIT2, cat.: 303516 or or M-T271, cat.: 356418), IgM (MHM-88, cat.: 314520), IgD (IA6-2, cat.: 348216), MHC2 (L243, cat.: 307610), IL-1β (H1B-27, cat.: 511604), mouse-IgG (Poly4053, cat.: 405317) or Zombie violet (cat.: 423113) (all from BioLegend); IFNAR (polyclonal, cat.: ab10739, Abcam); BCL-6 (K112-91, cat.: 561522/ 561525, BD); IL-21 (ebio3A3-N2, cat.: 50-7219, eBioscience); CD14 (TÜK4, cat.: 130-096-875, Miltenyi Biotec); CD38 (OKT 10, CRL-8022, ATCC); porcine monocyte-granulocyte (74-22-15 A, cat.: 561499), porcine CD3 (BB23-8E6-8C8, cat.: 561478), porcine CD4 (74-12-4-RUO, cat.: 561472), porcine CD8b (295/33-25, cat.: 561484) and porcine CD8a (76-2-11, cat.: 561475) (all from BD); IL-21 (polyclonal, cat.: orb9043, Biorbyt); porcine CD2 (MSA4, cat.: WS0590S-100) and porcine TCR1 δ (PGBL22A, cat.: WS0621S-100 (both from Kingfischer Biotech); porcine SLA class II DR (2E9/13, cat.: MCA2314F, AbD Serotec); porcine CD21 (BB6-11C9.6, cat.: SBA-4530-09, Southern Biotech); porcine IgM (polyclonal, cat.: AAI48B, Bio-Rad); and streptavidin (cat.: 25-4317-82), Foxp3 (FJK-16s, cat.: 48-5773-82) and T-bet (eBio4B10, cat.: 12-5825-82) (all from eBioscience). Fixable Viability Dyes (cat.: 65-0865-14 and 65-0866-14) were from eBioscience).

Neutralizing antibodies were as follows: anti-IL-6 (6708, cat.: MAB206-SP, R&D Systems), anti-IL-12 (B-T21, cat.: BMS152, eBioscience) and anti-TNF (MAb11, cat.: 502901, Biolegend), used at 10 μg/ml; and anti-IL-27 (307426, cat.: MAB25261 F, R&D Systems), used at 5μg/ml.

Recombinant cytokines were as follows: rIL-12 (eBioscience), used at 100 pg/ml; and rTNF, rIL-6 (eBioscience) and rIL-27 (R&D Systems), used at 10 ng/ml.

The following TLR ligands were purchased from Invivogen and were used at the following concentrations: CL075 (3M002; 1 μg/ml), LPS-EK Ultrapure (2 μg/ml), Pam_3CSK_4 (200 ng/ml), poly(I:C) LMW (2 μg/ml) and ODN 2395 (5 μM). Bacterial RNA was isolated from mid-log phase cultures of DH5alpha *E. coli* using Trizol (Life Technologies, Karlsruhe, Germany). Transfection of bacterial RNA into human monocytes was performed using polycationic polypeptide poly-L-arginine (pLa) (Sigma-Aldrich).

Enzyme-linked immunosorbent assay (ELISA). The concentration of TNF, IL-1β, IL-6, IL-10, IL-12p40, IL-23, GM-CSF and IL-27 in culture supernatants was measured by ELISA (all purchased from eBioscience) according to standard manufacturer's recommendations. Concentrations of IL-12p70 were measured using a human IL-12p70 High Sensitivity ELISA kit (eBioscience). The samples were analyzed for absorbance at 450 nm using FilterMax F5 Multi-Mode Microplate Reader (Molecular Devices). The concentration of porcine IL-12p40 and IL-6 in culture supernatants were measured by ProcartaPlex Pig Kit (eBioscience) or by Quantikine ELISA kit (R&D Systems), and results were collected using a Luminex MAGPIX instrument (Merck Millipore). Human IgG was determined by ELISA using polyclonal goat anti-human IgG (polyclonal, cat.: AHI0301, TAGO Immunologicals) and purified human IgG (purified from serum, cat.: I2511, Sigma) as standard. Results were collected on a Spark multimode reader (Tecan, Männedorf, Switzerland).

Anti–*S. enterica* IgG ELISA. 96-well microtiter plates were coated overnight with lysates of *S. enterica* serovar Typhimurium (Salmoporc-STM) (3μg/ml) that we generated from log-phase cultures of *Hys*$^-$*Ade*$^-$ *S. enterica*. Serum samples from immunized pigs were serially diluted (12 dilutions) and were incubated in the pre-coated plates for 12 h at 4 °C, followed by washing and incubation with affinity-purified polyclonal goat antibody to swine IgG labeled with HRP (goat anti-pig IgG (gamma)-HRP, SeraCare Life Sciences, cat.:5220-0363 14-14-06, polyclonal) for 1 h. Bound goat anti-pig IgG (gamma)-HRP was visualized by the addition of TMB substrate (Thermo Fisher), and the titer of antibodies to *S. enterica* for each animal was visualized as absorbance readings at 450 nm at a set serum dilution of 1 to 51,200.

RNA isolation. $CD14^+CD16^-$ human monocytes were sorted by flow cytometry and were infected with EC at MOI = 10 or stimulated with HKEC at 10:1 ratio of bacteria to cells. After 6 h, cells were harvested, washed once in PBS and lysed in Trizol (Life Technologies). Total RNA was prepared according to the manufacturer's suggested protocol.

Gene array. Total RNA was prepared from four independent experiments (four separate donors) according to the Trizol manufacturer's protocol. Samples were further purified on columns (RNeasy Micro Kit, Qiagen).

RNA integrity was checked on an Agilent 2100 Bioanalyser (Agilent Technologies) with 6000 Nano Chips. RNA was judged as suitable only if samples showed intact bands of 18 S and 28 S ribosomal RNA subunits, displayed no chromosomal peaks or RNA degradation products, and had a RNA integrity number (RIN) above 8.0.

100 ng RNA was used for whole-transcript cDNA synthesis with the Ambion WT expression kit (Life Technologies). Hybridization, washing and scanning

of an Affymetrix GeneChip Human Gene 1.1 ST 24-array plate was carried out according to standard Affymetrix protocols on a GeneTitan instrument (Affymetrix).

Quality control, normalization and statistical analysis were performed using MADMAX, a pipeline consisting of integrated Bioconductor packages[50]. Probe sets were redefined according a published article using current genome information[51]. Normalized gene-expression estimates were obtained from the raw intensity values by using the robust multiarray analysis preprocessing algorithm available in the library AffyPLM using default settings[52]. Only genes that were targeted by at least seven probes, reached $\log_2$ expression of > 4.32 on at least three microarrays and had a $\log_2$ interquartile range value of > 0.25 across all samples were considered for further analysis. Intensity-based moderated *t*-statistics were applied for pairwise comparisons to identify differentially regulated genes[53]. To correct for multiple testing, a false-discovery rate method was used to calculate *q* values[54]. A *q* value of < 0.01 was considered significant.

RNA-mediated interference. Silencer Select siRNA duplexes targeting TLR8 (sequence ID: s27920, s27921 and s27922), MyD88 (sequence ID: s9136, s9137 and s9138) and negative controls were obtained from Life Technologies. Monocytes cultured in 96-well plates were transfected with 25 nM of each siRNA using Viromer Blue transfection reagent (Lipocalyx) following manufacturer recommendations for sensitive cells and reverse transfection. Cells were plated at a density of 5×10^5 cells per ml in a final volume of 100 µl in 96-well plates. At 48 h after transfection, cells were infected or treated as described in the text or figure legends. Knockdown of TLR8 and Myd88 was confirmed 48 h after transfection of siRNA by RT-PCR using specific primers (TLR8: forward primer 5′-AGTTTCTCTTCTCGGCCACC-3′ and reverse primer, 5′-ACATGTTTTCCATGTTTCTGTTGT -3′, MyD88: forward primer 5′-TCTCCAGGTGCCCATCAGAA-3′ and reverse primer 5′-GGTTGGTGTAGTCGCAGACA-3′).

Four custom-designed Silencer Select siRNA duplexes targeting porcine TLR8 (combination of four siRNA duplexes) were purchased from Life Technologies, with the following sequences:

TLR8-1 sense: 5′-GCAAAUUGAUUUUACCAUUTT-3′;
antisense: 5′-AAUGGUAAAAUCAAUUUGCTT-3′;
TLR8-2 sense: 5′-GAUUUAAGCUUGAACAGUATT-3′;
antisense: 5′-UACUGUUCAAGCUUAAAUCTA-3′;
TLR8-3 sense: 5′-GCAUCUUUACUUUAACAGATT-3′;
antisense: 5′-UCUGUUAAAGUAAAGAUGCTG-3′;
TLR8-4 sense: 5′-CAAUAUUCGUUUUAACCAATT-3′;
antisense: 5′-UUGGUUAAAACGAAUAUUGTC-3′;

Porcine $CD14^+$ monocytes cultured in 96-well plates were transfected with 25 nM of each siRNA following the protocol described above for human cells. At 48 h after transfection, cells were infected or treated as described in the text or figure legends.

Flow cytometry and cell sorting. Flow cytometry regularly was performed on a BD FACSCanto II cytometer Data was analyzed using FlowJo software Version: 7.6.5 (Treestar).

$CD14^+CD16^-$ monocytes were sorted from PBMCs on a BD FACSAria II SORP cell sorter (BD Biosciences) $CD4^+CXCR5^+$ and $CD4^+CXCR5^-$ T cells were sorted from monocyte–T cell co-cultures on a BD FACSAria II SORP cell sorter. In vitro–generated T_{FH} cells were sorted on a FACSARIA II sorter as $CD19^-CD4^+CD45RA^-CXCR5^+$ cells, and naive T cells were sorted as $CD19^-CD4^+CD45RA^+$ cells. Memory B cells were sorted from human tonsils as $CD4^-CD19^+IgD^-CD38^-$ cells. Cell-purity checks were performed, and a purity of > 97% was confirmed.

QuantiGene Plex transcript analysis. Quantigene multiplex-plex assay (Affymetrix) was performed to quantify the expression of *GATA3*, *MAF*, *IL21*, *TBX21*, *RORC*, *FOXO1* and *BCL6* and two housekeeper genes (*ACTB* and *HPRT1*) according to the manufacturer's protocol. In brief, $CD4^+$ T cells were lysed at a concentration of 500 celld per microliter of lysis mixture supplemented with proteinase K and were incubated at 50 °C for 30 min before their addition to a hybridization plate. The hybridization plate was sealed with heat-sealing foil and was placed in a shaking incubator (VorTemp 56) at 54 ± 1 °C and 600 r.p.m. to allow the samples to hybridize for 18–22 h. Fluorescent bead signal detection was obtained using Bio-Plex Suspension Array System (Bio-Rad Laboratories). The mean fluorescence intensity for each probe was recorded.

Animal experiments. The animal experiments were performed in accordance with the Danish Animal Welfare Act under approval and authorization issued by the Danish Animal Experiment Inspectorate.

In total, 18 5-week-old pigs (Danish Landrace/Danish Yorkshire crossbreeds, paternal lineage Duroc) of both sexes, raised on a commercial farm (Bøgekærgård, Faxe, Denmark), were stratified by size (6.3–10.4 kg; average, 8.0 kg) and sex and were distributed into three groups. Animals in each group received 1 ml subcutaneous vaccination in the right side of the neck as follows: 1, live *Salmonella enterica* serovar Typhimurium vaccine (Salmoporc STM Ch.-B. 022 07 15, IDT Biologika) containing 3.32×10^8 CFU per dose, according to the product insert); 2, heat-inactivated (65° for 90 min) Salmoporc STM vaccine (HKST) using the same dose as in condition 1); or 3, saline alone. The live vaccine was administered within 2 h of reconstitution. The same immunization regimen was repeated as booster injections on day 14. Heat killing of the vaccine was confirmed by absence of bacterial growth on LB plates incubated at 37 °C for 24 h. Throughout the experiment, the pigs were housed in two adjoining boxes, each box housing equal numbers of animals from each of the three treatment groups. One pig in the live vaccine group was euthanized on day 19 of the experiment due to severe umbilical hernia unrelated to the vaccine. One pig in the control group developed fever, dyspnea and generalized fatigue on day 0 of the experiment and was suspected of having pneumonia; this pig was therefore treated successfully with 160 mg benzylpenicillin and 200 mg dihydrostreptomycin (0.8 ml Streptocillin Vet) over 3 consecutive days and was excluded from the analysis. Five animals per group were included in the final analyses.

Animals were killed according to regulations. Transverse sections of spleen and prescapular lymph node (LN, cervicalis superficialis dorsalis) draining from the injection site were fixated in 10% neutral-buffered formalin (4% formaldehyde, Pioneer Research Chemicals Ltd) for immunohistochemistry. The remaining LN and spleen tissues samples were homogenized using disposable scalpels, and single-cell suspensions were isolated by forcing homogenized tissue samples through a cell strainer (70 µm, Greiner Bio-One), followed by two washes with RPMI1640 and subsequent culture in RPMI1640 supplemented with 10% FCS (FCS), 1% glutamine, 1% HEPES buffer and 1% non-essential amino acids (all from Sigma-Aldrich).

For in vitro experiments reported in Fig. 6 and Supplementary Fig. 4, spleen samples were collected from German Landrace pigs of both sexes between 8 weeks and 1 year of age. Single-cell suspensions were prepared as described above.

Splenocytes were cultured in IMDM (Pan-Biotech) supplemented with 10% FCS and were stimulated with ST, HKST (MOI: 0.1, 0.5, 1, 3), LPS (2 µg/ml), CL075 (1 µg/ml) or pLa (280 ng) plus RNA (237 ng) in the presence of concavalin A (2 µg/ml) (Fisherscientific). After 1 h, penicillin-streptomycin (1%) was added. After 4 d, cells were restimulated with phorbol-12-myristat-13-acetat (PMA, 50 ng/ml) and ionomycin (1 µg/ml) (both obtained from Sigma) and then were harvested, washed and analyzed by flow cytometry. Live and dead cells were discriminated using Zombie Violet Fixable Viability Kit (Biolegend); dead cells were excluded from the analysis.

Immunohistochemistry. Spleen samples were immersion-fixed in formalin and embedded in paraffin and were cut into 2-µm sections for immunohistochemical analyses after dewaxing in xylene and rehydration in decreasing ethanol concentrations. For detection of PAX5, Ki67 and BCL22, heat-mediated antigen retrieval was performed in 10 mM citric acid (pH 6.0), microwaved at 600 W for 12 min. Spleen sections were incubated with a purified mouse monoclonal antibody to PAX5 (1:400, clone 24/Pax5, BD Biosciences) or BCL2 (1:100, LS-B2352, LSBio) or with a purified rabbit antibody monoclonal to Ki67 (1:150, clone SP6, Cell Marque) at 4 °C overnight. Incubation with an irrelevant immunopurified mouse antibody (Anti-MUC5b, ab77995, clone 19.4E, Abcam) or rabbit antibody (Anti-Villin, ab130751, clone SP145, Abcam) at the same dilution served as negative controls. Slides were incubated with the biotinylated secondary antibodies goat anti-mouse IgG (1:200, BA 9200, Vector) or goat anti-rabbit IgG (1:200, BA 1000, Vector) and HRP-coupled streptavidin. Diaminobenzidine (DAB) was used as substrate for color development. All slides were counterstained with hematoxylin, dehydrated through graded ethanol, were cleared in xylene and were coverslipped. Whole slide images of spleen tissues were generated by Aperio CS2 digital pathology scanner (Leica Biosystems Imaging).

Immunofluorescence. For immunofluorescent co-staining of PAX5 and Ki67, slides were incubated with the purified mouse monoclonal antibody to PAX5 (clone 24/Pax5, 610863, BD Biosciences,1:50) overnight at 4 °C as described above and with the Alexa Fluor 568–conjugated secondary antibody goat anti-mouse IgG (1:200, polyclonal, A-21124, Thermo Fisher Scientific) for 45 min at room temperature. Slides were then incubated with a purified rat antibody monoclonal to Ki67 (1:100, clone SolA15, eBioscience) at 4 °C overnight, then were incubated with the Alexa Fluor 488–conjugated secondary antibody goat anti-rat IgG (1:200, Thermo Fisher Scientific) for 45 min at room temperature and were mounted with Roti-Mount Fluor-Care DAPI (4,6-diaminidino-2-phenylindole, Carl Roth). Adequate negative controls, including incubation of slides with only one primary but both secondary antibodies, were conducted. Slides were analyzed by immunofluorescence microscopy with an Olympus BX41 microscope equipped with a DP80 camera (Olympus).

Case-control study. Samples of patients with TB and healthy volunteers were collected at Mahavir Hospital, Hyderabad (India); the generated cohort has been described before[55]. Informed consent was obtained from all subjects, and all investigations were conducted according to the principles of the Helsinki Declaration. Written approval was obtained from the research ethics board of the Central University of Hyderabad and Mahavir Hospital. Patients were enrolled in the Revised National Tuberculosis Control Program (RNTCP) of India, and recruited into the study on the day of treatment initiation (according to DOTS

strategy). Subjects positive for human immunodeficiency virus and those who had relapsed with TB were excluded from the cohort. The diagnosis of TB was based on clinical examination, chest X-ray, positive sputum test or histopathology. Healthy household contacts of the patients with TB were recruited as controls to ensure comparable exposure rates and environmental conditions. BCG-vaccination status was determined by the presence of a BCG-related skin scar. The cohort consisted of 293 patients and 165 control subjects. 61,4% of the patients with TB had pulmonary TB (PTB) and 38.6% had extra-pulmonary TB (ETB). The control subjects were significantly older (34.2 ± 9.3 years of age (mean ± s.e.m. throughout)) than the patients (25.4 ± 10.4 years of age; $t(456) = 8.787$; $P < 0.0001$) and had a significantly higher mean BMI (23.8 ± 4.9 (control) versus 18.0 ± 4.1 (patient); $t(292.8) = 12.995$; $P < 0.0001$). Sex distribution did not differ significantly between control subjects (59.4% females) and patients (61.8% females). The differences in age and BMI were corrected for through the use of a binary logistic regression model.

SNP analysis. DNA was extracted from buccal swabs of all study subjects using a FlexiGene DNA extraction Kit (Qiagen). *TLR8* SNPs were analyzed by real-time PCR on a Light Cycler instrument (Roche) using the following PCR primer sets:
forward 5′-TCAGGAAGTTAGCCAGTTTCTC-3′,
reverse 5′-CCTGCATTTACAGTTGTTTCGAT-3′,
sensor 5′-AAATAGAAGTGGCTTACCACGTTTCTG-3′T-FITC,
anchor Cy5-5′-TTCTAATTTTTCATTCCGTAACTTGCAGCAGCGCA-3′.
On the basis of previous observations that the presence of an A nucleotide defines the functionality, we defined the A/AA/AG as the allele encoding TLR8-A, and G/GG as the status of the allele encoding TLR8-G for our analysis.

Statistical analysis. Statistical analyses of in vitro experiments were performed using one-way ANOVA and Holm-Sidak's multiple comparisons test, or two-way ANOVA, or Wilcoxon's matched-pairs signed-rank test, or linear-regression analysis where appropriate. Calculations were performed using GraphPad Prism 6 Software (GraphPad Software).

For all statistical analysis, a P value of < 0.05 was considered statistically significant. 95% confidence intervals are provided in squared brackets in Supplementary Tables 3 and 4 (as '[CI 95%]'). Baseline characteristics of the study population were analyzed using Atudent's t-test or Pearson's chi-squared (χ^2) test. *TLR8* allele frequencies were compared using binary logistic regression, summarizing recessive genotypes and adjusting for age, BMI and sex. The interaction between BCG stats and TLR8-A or TLR8-G was assessed using Wald's statistics. Statistical tests were performed using IBM SPSS Statistics 21 software and figures were generated using GraphPad Prism 6 Software.

Life Sciences Reporting Summary. Further information on experimental design is available in the Life Sciences Reporting Summary.

Data availability. The datasets generated during and/or analyzed during the current study are available from the corresponding author on reasonable request. The gene array data are publicly available in the Gene Expression Omnibus database (accession code GSE68255).

References

50. Lin, K. et al. MADMAX - Management and analysis database for multiple ~omics experiments. *J. Integr. Bioinform.* **8**, 160 (2011).
51. Dai, M. et al. Evolving gene/transcript definitions significantly alter the interpretation of GeneChip data. *Nucleic Acids Res.* **33**, e175 (2005).
52. Irizarry, R. A. et al. Exploration, normalization, and summaries of high density ol array probe level data. *Biostatistics* **4**, 249–264 (2003).
53. Sartor, M. A. et al. Intensity-based hierarchical Bayes method improves testing for differentially expressed genes in microarray experiments. *BMC Bioinformatics* **7**, 538 (2006).
54. Storey, J. D. & Tibshirani, R. Statistical significance for genomewide studies. *Proc. Natl. Acad. Sci. USA* **100**, 9440–9445 (2003).
55. Dittrich, N. et al. Toll-like receptor 1 variations influence susceptibility and immune response to Mycobacterium tuberculosis. *Tuberculosis (Edinb.)* **95**, 328–335 (2015).

nature research

Corresponding author(s): Leif Erik Sander (leif-erik.sander@charite.de)

☐ Initial submission ☐ Revised version ☒ Final submission

Life Sciences Reporting Summary

Nature Research wishes to improve the reproducibility of the work that we publish. This form is intended for publication with all accepted life science papers and provides structure for consistency and transparency in reporting. Every life science submission will use this form; some list items might not apply to an individual manuscript, but all fields must be completed for clarity.

For further information on the points included in this form, see Reporting Life Sciences Research. For further information on Nature Research policies, including our data availability policy, see Authors & Referees and the Editorial Policy Checklist.

Experimental design

1. Sample size

Describe how sample size was determined.

Sample size was chosen based on previous experience. Relevant data for accurate power calculation was unavailable. A sample size of 3-8 was sufficient to detect statistically significant differences between experimental groups.

2. Data exclusions

Describe any data exclusions.

Outliers were identified using appropriate statistical outlier-tests using Graph Pad Prism Software.
In the animal study, one pig in the live vaccine group was excluded due to a severe umbilical hernia, unrelated to the vaccine. One pig in the control group presented on day 0 of the experiment with fever, dyspnea and generalized fatigue, suspected of pneumonia and was excluded from the analysis. Five animals per group were included in the final analyses.
One individual was excluded from the case-control study due to unclear vaccination status.

3. Replication

Describe whether the experimental findings were reliably reproduced.

All the reported experiments were reproducible, as shown by independent experiments.

4. Randomization

Describe how samples/organisms/participants were allocated into experimental groups.

For in vivo experiments, animals were stratified by age, sex, and size and weight.

5. Blinding

Describe whether the investigators were blinded to group allocation during data collection and/or analysis.

Experimentators where blinded regarding the treatement groups of the animal experiment.

Note: all studies involving animals and/or human research participants must disclose whether blinding and randomization were used.

6. Statistical parameters

For all figures and tables that use statistical methods, confirm that the following items are present in relevant figure legends (or in the Methods section if additional space is needed).

n/a	Confirmed
☐	☒ The exact sample size (*n*) for each experimental group/condition, given as a discrete number and unit of measurement (animals, litters, cultures, etc.)
☐	☒ A description of how samples were collected, noting whether measurements were taken from distinct samples or whether the same sample was measured repeatedly
☐	☒ A statement indicating how many times each experiment was replicated
☐	☒ The statistical test(s) used and whether they are one- or two-sided (note: only common tests should be described solely by name; more complex techniques should be described in the Methods section)
☐	☒ A description of any assumptions or corrections, such as an adjustment for multiple comparisons
☐	☒ The test results (e.g. *P* values) given as exact values whenever possible and with confidence intervals noted
☐	☒ A clear description of statistics including central tendency (e.g. median, mean) and variation (e.g. standard deviation, interquartile range)
☐	☒ Clearly defined error bars

See the web collection on statistics for biologists for further resources and guidance.

Software

Policy information about availability of computer code

7. Software

Describe the software used to analyze the data in this study.	FlowJo version 9, MADMAX, ProSA, PROCHECK, ERRAT, CASTp, ProFunc, WEBnm, ElNemo,I-Mutant 2.0, MutPred, FoldX, GraphPad Prism 6, R (JMP statistics software), MS Excel.

For manuscripts utilizing custom algorithms or software that are central to the paper but not yet described in the published literature, software must be made available to editors and reviewers upon request. We strongly encourage code deposition in a community repository (e.g. GitHub). *Nature Methods* guidance for providing algorithms and software for publication provides further information on this topic.

Materials and reagents

Policy information about availability of materials

8. Materials availability

Indicate whether there are restrictions on availability of unique materials or if these materials are only available for distribution by a for-profit company.	There are no restrictions on the availability of any materials used in this study

9. Antibodies

Describe the antibodies used and how they were validated for use in the system under study (i.e. assay and species).

All the antibodies are from commercial sources and have been validated by the vendors. Validation data are available on the manufacturer's website.
Antibodies for flow cytometry: CD3 (UCHT1, cat.: 300415), CD4 (OKT4, cat.: 317424), IFNγ (4S.B3, cat.: 502528), IL17 (BL168, cat.: 512306), CXCR5 (J252D4, cat.: 356904), PD1 (EH12.2H7, cat.: 329922), ICOS (C398.4A, cat.: 313510), CD19 (HIB19, cat.: 302228 or SJ25C1, cat.: 363022), CD20 (2H7, cat.: 302324), CD27 (O323, cat.: 302810), CD38 (HIT2, cat.: 303516 or or M-T271, cat.: 356418), IgM (MHM-88, cat.: 314520), IgD (IA6-2, cat.: 348216), MHC2 (L243, cat.: 307610), anti IL-1b (H1B-27, cat.: 511604), Zombie violet (cat.: 423113;(all from Biolegend, San Diego, CA). Anti IFNar (polyclonal , cat.: ab10739, Abcam, Cambridge, UK), BCL6 (K112-91, cat.: 561522/ 561525, BD, Franklin Lake, NJ), IL-21 (ebio3A3-N2, cat.: 50-7219, eBioscience), CD14 (TÜK4, cat.: 130-096-875, Miltenyi Biotec, Bergisch Gladbach, Germany), CD38 (OKT 10, CRL-8022, ATCC, Manassas, VA).porcine Monocyte/Granulocyte (74-22-15A, cat.: 561499, BD, Franklin Lake, NJ), porcine CD3 (BB23-8E6-8C8, cat.: 561478), porcine CD4 (74-12-4-RUO, cat.: 561472, BD), porcine CD8b (295/33-25, cat.: 561484, BD), IL-21 (polyclonal, cat.: orb9043, Biorbyt, San Francisco, CA) porcine CD8a (76-2-11, cat.: 561475, BD), porcine CD2 (MSA4, cat.: WS0590S-100, Kingfischer Biotech), porcine SLA Class II DR (2E9/13, cat.: MCA2314F, AbD Serotec), porcine CD21 (BB6-11C9.6, cat.: SBA-4530-09, Southern Biotech), porcine TCR1 δ (PGBL22A, cat.: WS0621S-100, Kingfischer Biotech), mouse-IgG (Poly4053, cat.: 405317, Biolegend), porcine IgM (polyclonal, cat.: AAI48B, Bio-Rad), Streptavidin (cat.: 25-4317-82, eBioscience), Foxp3 (FJK-16s, cat.: 48-5773-82, eBioscience), Tbet (eBio4B10, cat.: 12-5825-82, eBioscience). Fixable Viability Dyes (cat.: 65-0865-14 and 65-0866-14, eBioscience).

Immunohistochemistry and immunofluorescence: mouse monoclonal AB to PAX5 (1:400, 24/Pax5, BD Biosciences), BCL2 (1:100, LS-B2352, LSBio, Seattle, WA, USA), purified rabbit monoclonal to KI67 (1:150, SP6, Cell Marque, Rocklin, CA). Goat anti-mouse IgG (1:200, BA 9200, Vector Burlingame, CA) or goat anti-rabbit IgG (1:200, BA 1000, Vector, Burlingame, CA). Alexa-568-goat anti-mouse IgG (1:200, Thermo Fisher Scientific, Darmstad, Germany) Alexa-488-goat anti-rat IgG(1:200, Thermo Fisher Scientific).

Neutralizing antibodies: anti-IL-6 (6708, cat.: MAB206-SP, R&D Systems, Minneapolis, MN), anti-IL-12 (B-T21, cat.: BMS152, eBioscience) and anti-TNFα (MAb11, cat.: 502901, Biolegend) were used at 10μg/ml. Anti-IL-27 (307426, cat.: MAB25261 F, R&D Systems) was used at 5μg/ml.

10. Eukaryotic cell lines

a. State the source of each eukaryotic cell line used.

HEK-Blue Null-I cells were purchased from Invivogen (Toulouse, France)

b. Describe the method of cell line authentication used.

The cell line was purchased directly from the vendor and used for experiments. Independent authentication was not performed.

c. Report whether the cell lines were tested for mycoplasma contamination.

All cell lines tested negative for mycolplasma contamination

d. If any of the cell lines used are listed in the database of commonly misidentified cell lines maintained by ICLAC, provide a scientific rationale for their use.

No commonly misidentified cell lines were used in this study

Animals and human research participants

Policy information about studies involving animals; when reporting animal research, follow the ARRIVE guidelines

11. Description of research animals

Provide details on animals and/or animal-derived materials used in the study.

Salmonella vaccination study: Five-week-old pigs (Danish Landrace/Danish Yorkshire crossbreeds, paternal lineage Duroc) of both sexes, raised on a commercial farm (Bøgekærgård, Faxe, Denmark) were stratified by size (6.3 to 10.4 kg, averaging 8.0 kg) and sex, and distributed to three groups.
BCG vaccination study: Five-weeks old female pigs (Danish Landrace/Danish Yorkshire crossbreds and paternal Duroc) rasied on a commercial farm (Askelygård, Roskilde, Denmark) were stratified by size (total weight range 5.5-11.5 kg, averaging 8.9 kg) and distributed to two groups.

12. Description of human research participants

Describe the covariate-relevant population characteristics of the human research participants.

Samples of TB patients and healthy volunteers were collected in Mahavir Hospital, Hyderabad (India) and the generated cohort has been described before.
HIV-positive and relapse cases were excluded from the cohort. TB diagnosis was based on clinical examination, chest X-Ray, positive sputum test or histopathology. Healthy household contacts of the TB patients were recruited as controls, to ensure comparable exposure rates and environmental conditions. BCG vaccination status was determined by the presence of a BCG-related skin scar. The cohort consisted of 293 patients and 165 controls.
61,4% of the TB patients had pulmonary TB (PTB) and 38.6% Extra-pulmonary TB (ETB). Controls were significantly older (mean=34.2±9.3) than patients (mean=25.4 ±10,4;$t(456)= 8.787;p<0.0001$) and had a significantly higher mean BMI (mean=23.8±4.9 and mean=18.0±4.1 respectively, $t(292.8)=12.995;p<.0001$). Gender distribution did not differ significantly between controls (59.4% females) and patients (61.8% females). The age and BMI differences were corrected for using a binary logistic regression model.

Corresponding author(s): Leif Erik Sander (leif-erik.sander@charite.de)

☐ Initial submission ☐ Revised version ☒ Final submission

Flow Cytometry Reporting Summary

Form fields will expand as needed. Please do not leave fields blank.

Data presentation

For all flow cytometry data, confirm that:

☒ 1. The axis labels state the marker and fluorochrome used (e.g. CD4-FITC).

☒ 2. The axis scales are clearly visible. Include numbers along axes only for bottom left plot of group (a 'group' is an analysis of identical markers).

☒ 3. All plots are contour plots with outliers or pseudocolor plots.

☒ 4. A numerical value for number of cells or percentage (with statistics) is provided.

Methodological details

5. Describe the sample preparation.	Leukocytes were isolated from human and porcine blood through density centrifugation and cellular populations of interest were purified via immunomagnetic separation or FACS based sorting. Porcine spleen were processed through a cell strainer to obtain single cells suspensions, and CD4+ T cells, CD14+CD172+ monocytes, and CD14-CD172+ DC were isolated by FACS sorting.
6. Identify the instrument used for data collection.	Flow cytometry was regularly performed on a BD FACS Canto II cytometer provided by the flow cytometry core at the BCRT, Charité Berlin.
7. Describe the software used to collect and analyze the flow cytometry data.	Data were analyzed using FlowJo software (Treestar, San Carlos, CA).
8. Describe the abundance of the relevant cell populations within post-sort fractions.	Cell purity was routinely checked by flow cytometry and only purities of >85% (monocytes) and >95% T and B cells were used for subsequent experiments
9. Describe the gating strategy used.	Unless stated otherwise, all flow cytometric analysis was carried out after pre-gating on viable cells by morphology (FSC/SSC) and indicator dye staining, and exclusion of doublets (FSC-A/FSC-H, SSC-A/FSC-H). Downstream gating is specified in the figure legends.

Tick this box to confirm that a figure exemplifying the gating strategy is provided in the Supplementary Information. ☒